International Institute for
Applied Systems Analysis
Schlossplatz 1
A-2361 Laxenburg, Austria

Tel: +43 2236 807 342
Fax: +43 2236 71313
E-mail: publications@iiasa.ac.at
Web: www.iiasa.ac.at

Interim Report IR-10-027

Ecological factors driving the long-term evolution of influenza's host range

Sarah Cobey (scobey@hsph.harvard.edu)
Mercedes Pascual (pascual@umich.edu)
Ulf Dieckmann (dieckmann@iiasa.ac.at)

Approved by

Detlof Von Winterfeldt
Director

July 2011

Interim Reports on work of the International Institute for Applied Systems Analysis receive only limited review. Views or opinions expressed herein do not necessarily represent those of the Institute, its National Member Organizations, or other organizations supporting the work.

Ecological factors driving the long-term evolution of influenza's host range

Sarah Cobey[1]*, Mercedes Pascual[1,2], and Ulf Dieckmann[3]

[1]*Department of Ecology and Evolutionary Biology, 830 North University Avenue,*
University of Michigan, Ann Arbor, Michigan 48109, USA
[2]*Howard Hughes Medical Institute, USA*
[3]*Evolution and Ecology Program, International Institute for Applied Systems Analysis*
(IIASA), Schlossplatz 1, A-2361 Laxenburg, Austria

*Author and present address for correspondence: Center for Communicable Disease Dynamics, Harvard School of Public Health, 677 Huntington Avenue, Boston, MA 02115, USA (scobey@hsph.harvard.edu)

Abstract

The evolution of a pathogen's host range is shaped by the ecology of its hosts and by the physiological traits that determine host specificity. For many pathogen traits there is a tradeoff: a phenotype suitable for infecting one set of hosts poorly infects another. Introducing and analyzing a simple evo-epidemiological model, here we study how such a tradeoff is expected to affect evolution of the host ranges of influenza viruses. We examine a quantitative trait underlying host specificity, given by an influenza virus's degree of adaptation to certain conformations of sialic acid receptors, and investigate how this receptor preference evolves in a minimal network of host species, including humans, that differ in life history and receptor physiology. Using adaptive dynamics theory, we establish thresholds in interspecific transmission rates and host population sizes that govern the emergence and persistence of human-adapted viruses. These ecological thresholds turn out to be largely independent of the strength of the evolutionary tradeoff, underscoring the importance of ecological conditions in determining a disease's host range.

Keywords: influenza; host range; adaptive dynamics; emerging infectious diseases

1. INTRODUCTION

Several challenges complicate the task of predicting evolution. One is the presence of evolutionary constraints: It may not be possible to optimize two phenotypic traits simultaneously, because a high value in one trait rules out high values in the other. Another problem concerns attainability: Evolutionary pathways may lead through regions of low fitness or, if mutations interact epistatically, may be difficult to map to phenotypes in the first place. Yet another class of problems arises from the environment or ecology in which evolution occurs: The fitness of a trait may be frequency-dependent, being influenced by the phenotypes of other individuals. Fitness can also be affected by population size, spatial interactions, and extrinsic factors, and these relationships can be nonlinear and dynamic.

Predicting evolution of host ranges in pathogens requires confronting several of these problems at once. Many pathogens show adaptations to specific host or tissue types and are unable to infect other hosts or tissues without undergoing extensive adaptation (Baranowski et al. 2001; Webby et al. 2004). Such adaptation often comes at the expense of the ability to infect an original host type, and thus presents an evolutionary constraint in the form of a tradeoff. Pathogens tend to undergo extreme changes in population size during the same period in which rapid evolution occurs. Host immunity and host demography furthermore often impose frequency-dependent selection.

Given this complexity, it is not surprising that there is little general theory for the evolution of host ranges in pathogens. This is unfortunate, considering the ubiquity of zoonoses: Most pathogens of humans infect at least one other species (Woolhouse &

Gowtage-Sequeria 2005). Existing models address host range indirectly. For example, Parker (2003) used optimization principles to show how parasitic helminths may expand their host range through trophic transmission to acquire complex life cycles. Gandon (2004) developed predictions for the evolution of virulence and transmission in a multihost environment. Some insights might also be gained by interpreting host range as a resource-choice problem for pathogens. In Levins's (1962) classic approach, consumers are predicted to specialize under strong tradeoffs and to adopt generalist strategies when tradeoffs are weak. His model, like Parker's, assumes that the optimal strategy will prevail. When selection is frequency-dependent, however, optimization principles are likely to give qualitatively incorrect predictions (Dieckmann et al. 2002; Egas et al. 2004; Koelle et al. 2005).

Our goal in this study is to develop basic predictions for the evolution of influenza's host range. Host range here refers to the specificity and diversity of pathogens in the host community. We choose influenza because of its importance to the health of animal populations and its interesting constraints and ecology. At the same time, the methods of analysis presented here are general and might be of interest also with regard to many other pathogens. Our analysis focuses on how host ecology and a tradeoff in host specialization are expected to influence evolutionary outcomes in the long run. We do not consider the mechanistic details of evolutionary attainability here, since the genotype-to-phenotype maps relevant to influenza's host range are poorly known (Baigent & McCauley 2003). Like Levins's approach, ours ignores environmental variation, such as seasonality, and assumes that viral population dynamics roughly equilibrate between successful invasions of pathogen strategies. These simplifications allow us to obtain general results about the structure of host ranges in a heterogeneous host environment, when adaptation is restricted by a single evolutionary constraint. We find that (i) specialists are favored for a broad range of both weak and strong tradeoffs, (ii) the scope for specialist coexistence sensitively depends on interspecific transmission rates and host population sizes, whereas (iii) these dependencies are only weakly affected by tradeoff strength.

2. BACKGROUND

The host range of many viruses is constrained by cell recognition (Baranowski et al. 2001). Influenza viruses all bind to cell-surface oligosaccharides with a terminal sialic acid. Sialic acids fall into one of two general types of conformations: the Neu5Acα(2,3)-Gal linkage or the Neu5Acα(2,6)-Gal linkage. The intestinal and/or respiratory epithelia of waterfowl, horses, and dogs contain mainly cells with α2,3-linked sialic acids, whereas the upper respiratory epithelia of cats and humans are dominated by α2,6-linked sialic acid receptors (Baigent & McCauley 2003). Pigs, the alleged "mixing vessels" of influenza viruses (Webster et al. 1992), contain both types of receptors in their respiratory tracts (Scholtissek et al. 1998). Chickens also possess both types of receptors (Gambaryan et al. 2002). Experiments have shown that most viruses cannot replicate in host tissue of dissimilar receptor type, and viruses preferring one receptor type can often sustain some replication in any host possessing that type, even if they are adapted to another species (e.g., Ito et al. 1999; Kida et al. 1994). Thus, the chemistry of receptor binding creates a tradeoff between the ability of influenza viruses to invade cells of one type or the other.

The distribution of α2,3- and α2,6-linked receptors in the host community presents an interesting evolutionary challenge: In a population of diverse potential hosts, under what circumstances will viruses evolve new receptor preferences? The emergence of avian influenza subtype H5N1 in humans has been ascribed to high interspecific mixing in backyard farms, large population sizes in the expanding commercial poultry industry, and the presence of intermediate hosts (pigs or chickens) that serve as ecological and evolutionary bridges between waterfowl and humans (Bulaga et al. 2003; Liu et al. 2003; Webster 2004; Webster & Hulse 2004). How easily could α2,6-adapted mutant viruses invade in these different environments, and would they be able to coexist in the long run with α2,3-adapted resident viruses?

Here we analyze how the host range of influenza changes with tradeoff strength in a simple evo-epidemiological model in which influenza viruses can adapt their receptor preference. We first assume that host species are epidemiologically equivalent except for their receptor types. Subsequently, we adopt more realistic assumptions and explore how the evolutionary dynamics of influenza viruses are modulated by two major components of influenza's ecology, interspecific transmission rates and the relative abundances of different host species.

3. METHODS

(a) *Epidemiological dynamics*

We consider a community with three host populations. One population, with abundance N_r, represents the waterfowl reservoir and has only α2,3-receptors. Another population, with abundance N_t, represents the "target" population (e.g., cats or humans) and has only α2,6-receptors. The third population, with abundance N_m, represents intermediate hosts such as pigs and chickens that possess both receptor types. We assume there are contacts between the reservoir and intermediate hosts (N_r and N_m) and between the intermediate and target hosts (N_m and N_t), but not between the reservoir and the target hosts (figure 1*a*).

Whether a contact between infected and susceptible host individuals results in transmission of the influenza virus depends on the host's receptor type and the virus's receptor preference p. We define p as the virus's probability of infecting via an α2,6-receptor; a perfect α2,6-specialist thus has $p = P(\alpha2,6) = 1$. In our model, the virus's probability of infecting via an α2,3-receptor, $P(\alpha2,3)$, is related to $P(\alpha2,6)$ through a tradeoff with strength s (Egas et al. 2004),

$$P(\alpha 2,3)^{1/s} + P(\alpha 2,6)^{1/s} = 1 \ . \tag{1}$$

This tradeoff can be tuned to be weak ($s < 1$) or strong ($s > 1$). For later reference, we introduce three broad categories of viral phenotypes: α2,6-specialists, α2,3-specialists, and generalists. We consider an α2,6-specialist to have a low degree of specialization if $0.5 < P(\alpha2,6) - P(\alpha2,3) < 0.8$ and a high degree of specialization if $P(\alpha2,6) - P(\alpha2,3) \geq 0.8$. The criteria for α2,3-specialization are analogous. A virus is considered adapted to a receptor if it is specialized to that receptor. Generalist preferences comprise the remaining cases, $|P(\alpha2,6) - P(\alpha2,3)| \leq 0.5$ (figure 1*b*).

Epidemiological dynamics follow the susceptible-infected-recovered-susceptible (SIRS) model. The transition of a host from recovered to susceptible indirectly captures two kinds of processes, the replenishment of susceptible hosts via births and deaths and the loss of immunity due to antigenic evolution by the pathogen. Our model represents these dynamics by six ordinary differential equations. The equations follow the rates $\mathrm{d}S/\mathrm{d}t$ and $\mathrm{d}I/\mathrm{d}t$ at which the abundances of susceptible and infected hosts change in each of the three host populations. Since we assume constant population sizes, the rates $\mathrm{d}R/\mathrm{d}t$ at which the number of recovered hosts changes in each of the three host populations follow from those equations. For each host in population i = r ("reservoir"), m ("intermediate"), t ("target"), the rate of susceptible replenishment is given by γ_i, the rate of infection by λ_i, and the rate of recovery by ν_i. Below we explicitly show the equations for each state of the intermediate host,

$$\frac{\mathrm{d}S_\mathrm{m}}{\mathrm{d}t} = \gamma_\mathrm{m} R_\mathrm{m} - \lambda_\mathrm{m} S_\mathrm{m} \ , \tag{2a}$$

$$\frac{\mathrm{d}I_\mathrm{m}}{\mathrm{d}t} = \lambda_\mathrm{m} S_\mathrm{m} - \nu_\mathrm{m} I_\mathrm{m} \ , \tag{2b}$$

$$\frac{\mathrm{d}R_\mathrm{m}}{\mathrm{d}t} = \nu_\mathrm{m} I_\mathrm{m} - \gamma_\mathrm{m} R_\mathrm{m} \ . \tag{2c}$$

The force of infection in the intermediate host, λ_m, equals the sum of the per capita rates of acquiring infections from contacts with infected members of all host populations, $\lambda_\mathrm{m} = \lambda_\mathrm{mr} + \lambda_\mathrm{mm} + \lambda_\mathrm{mt}$. We initially assume that transmission rates are frequency-dependent (Keeling & Rohani 2007). This leads to the following form of the transmission term, illustrated here for the rate of new infections in the intermediate host caused by contact with reservoir hosts,

$$\lambda_{\mathrm{mr}} S_{\mathrm{m}} = \max[P(\alpha 2,3), P(\alpha 2,6)] \beta_{\mathrm{mr}} \left(\frac{c_{\mathrm{mr}} S_{\mathrm{m}}}{N_{\mathrm{r}} + c_{\mathrm{mr}} N_{\mathrm{m}}} \right) I_{\mathrm{r}}, \tag{3}$$

where β_{ij} is the baseline rate at which an infected individual in host population j transmits infection to a susceptible individual in host population i. The transmission rate β_{ij} takes into account physical and behavioral differences between the host populations that affect the likelihood of infection given a contact. The effective transmission rate between two different populations is further modified by the appropriate receptor probability [in equation (3), $\max[P(\alpha 2,3),P(\alpha 2,6)]$], and the fraction of contacted hosts that are susceptible [in equation (3), $(\frac{c_{\mathrm{mr}} S_{\mathrm{m}}}{N_{\mathrm{r}} + c_{\mathrm{mr}} N_{\mathrm{m}}})$]. To specify this susceptible fraction, we introduce c_{mr}, the ratio of the probabilities per unit time of inter-population (between intermediate and reservoir hosts) and intra-population (among reservoir hosts) contact. The denominator, $N_{\mathrm{r}} + c_{\mathrm{mr}} N_{\mathrm{m}}$, is thus proportional to the expected total number of hosts contacted by an infected reservoir host during a given time period, and the numerator, $c_{\mathrm{mr}} S_{\mathrm{m}}$, is proportional to the expected number of susceptible intermediate hosts contacted by an infected reservoir host during the same time period.

For simplicity, we initially assume $c_{ij} = c_{ji} = c$, before relaxing this assumption later. Under this assumption, c controls the degree of mixing between host populations. For $c = 0$, all contacts occur within the separate host populations. In this situation, if $S_i/N_i \approx 1$, the effective transmission rate equals the baseline rate β_{ii}, and no contacts are potentially wasted on hosts in other populations. The case $c = 1$ implies free mixing between reservoir and intermediate hosts and between intermediate and target hosts. As c

approaches infinity, the effective transmission rate between host populations *i* and *j* equals β_{ij} (again assuming $S_i/N_i \approx 1$), and the effective transmission rate within host populations drops to zero. A more restrictive interpretation of our parameterization is that c_{ij} represents the fraction of population *j* in the range of population *i*, implying $c \in [0,1]$; c_{ij} can also be interpreted as the integrated product of the spatial frequency distributions for hosts *i* and *j*. We further assume that the between-population transmission rates β_{ij} equal the average of the two corresponding within-population transmission rates,

$$\beta_{ij} = \beta_{ji} = \frac{\beta_{ii} + \beta_{jj}}{2}. \tag{4}$$

Extending these conventions to infections arising from contacts with infected hosts from all three host populations, we obtain,

$$\lambda_{\mathrm{m}} = \max[P(\alpha 2,3), P(\alpha 2,6)]\left(\frac{\beta_{\mathrm{mr}} c_{\mathrm{mr}} I_{\mathrm{r}}}{N_{\mathrm{r}} + c_{\mathrm{mr}} N_{\mathrm{m}}} + \frac{\beta_{\mathrm{mm}} I_{\mathrm{m}}}{c_{\mathrm{mr}} N_{\mathrm{r}} + N_{\mathrm{m}} + c_{\mathrm{mt}} N_{\mathrm{t}}} + \frac{\beta_{\mathrm{mt}} c_{\mathrm{mt}} I_{\mathrm{t}}}{c_{\mathrm{mt}} N_{\mathrm{m}} + N_{\mathrm{t}}}\right). \tag{5}$$

Equations for the other host populations are analogous (equations S1 and S2). As equation (5) illustrates, in our model infection of the intermediate host occurs via the receptor type to which the infecting virus is better adapted. By modeling all mortality implicitly in the rate of susceptible replenishment, our model assumes that infections are acute and do not kill hosts, and that natural mortality acts only on recovered hosts.

(b) *Evolutionary dynamics*

To model the evolution of host range, we test the ability of a mutant virus with receptor preference p_1 to invade a community of hosts infected with a resident virus of receptor preference p_2. To constrain the problem, we assume that in each host population, the resident virus has reached its endemic equilibrium, and that the ability of the mutant to invade the resident is given by its instantaneous growth rate when rare in the environment determined by the resident. This growth rate, also known as the mutant's invasion fitness in the resident's environment (Metz et al. 1992), is given by the dominant eigenvalue of the Jacobian of the rare mutant's epidemiological dynamics (electronic supplementary material). The endemic equilibrium and the dominant eigenvalue are calculated numerically, since both are determined by polynomial equations of orders in excess of four.

By determining the growth rate of every possible mutant phenotype against every possible resident phenotype, we obtain pairwise invasibility plots (PIPs). PIPs show which phenotypes are uninvasible once attained and which phenotypes can be attained through the succession of small and advantageous mutational steps. The former phenotypes are called evolutionarily stable, the latter convergence stable. Our assumptions and approach are an application of the theory of adaptive dynamics (Dieckmann & Law 1996; Geritz et al. 1998; Metz et al. 1996).

4. RESULTS

(a) *Effects of tradeoff strength in a neutral host ecology*

We first examine how host range evolves when the host populations are epidemiologically equivalent in every respect but their receptors: hosts share the same population sizes and rates of contact, recovery, and susceptible replenishment, but their receptors vary. For simplicity, we assume $c = 1$, implying free mixing between reservoir and intermediate hosts and between intermediate and target hosts.

For very weak tradeoffs ($s \leq 0.5$ in figure 2*a*), a complicated dynamic emerges. The PIPs show two strategies that are both evolutionarily and convergence stable, but only locally. Which strategies are realized depends on the phenotype of the initial resident and on the mutational step size. For $s = 0.5$, starting from a perfect α2,3-specialist (i.e., from a resident with $p = 0$), mutants that are slightly better adapted to the target host than the residents can invade up to $p \approx 0.23$ (where $P(\alpha 2,3) \approx 0.97$). If mutations are always small, this resident, which shows a low degree of α2,3-specialization, will persist indefinitely. However, there is evidence that in some subtypes of influenza viruses, single mutations can effect large changes in receptor binding. If mutations are large, mutants with sufficiently high p can still invade when tradeoffs are very weak. At $s = 0.5$, invasions by mutants with very high p leads to a resident strategy at $p \approx 0.97$ (where $P(\alpha 2,3) \approx 0.23$, corresponding to low α2,6-specialization). This other attractor is also locally evolutionarily and convergence stable.

As the tradeoff strengthens, the two local attractors disappear, and only the repellor previously separating them remains. The two perfect specialists (at $p = 0$ and $p = 1$) thus become evolutionary end points. If mutational step sizes are small, only one perfect specialist will arise from a given starting condition. For example, if $s = 0.75$, a resident starting at $p = 0.5$ can be progressively invaded by mutants with smaller p until arriving at perfect α2,3-specialization. As before, which specialist appears depends on the phenotype of the initial resident. Figure 2 also shows that if mutational step sizes are large, a mutant better adapted to α2,6-receptors (i.e., with $P(\alpha 2,6)$ above ≈ 0.7) can invade a perfect α2,3-specialist and evolve increasing α2,6-specialization, and vice versa.

Assuming that large mutations can occur and that multiple specialists are able to arise, will they coexist? Reflecting the plots about their main diagonal reveals areas of mutual invasibility, or protected dimorphic coexistence: both the mutant and the resident have positive invasion fitness in the environment of the other type. Evaluating the selection gradient in the regions of coexistence shows whether this coexistence is transient or evolutionarily stable. When the tradeoff is very weak ($s = 0.05$, 0.25, and 0.5), we see the basins of attraction for the equilibria described previously (figure 2*b*). In addition, we find a third attractor within the region of coexistence that is also locally evolutionarily stable. This kind of attractor is sometimes referred to as a singular coalition (Geritz et al. 1998). At $s = 0.5$, this attractor occurs where one resident is highly α2,6-specialized and the other is highly α2,3-specialized. For stronger tradeoffs ($s = 0.75$ and above), this attractor is absent, and perfect specialists can coexist as evolutionary end points.

In summary, if large mutations are possible, a neutral ecology almost always gives rise to pairs of specialists that are able to coexist in the long run; generalists only appear when the tradeoff is extremely weak ($s = 0.05$). These results appear robust for reasonable variations in ecological parameters (figures S1 and S2). Our analysis up to this point reveals additional features of the evolution of host range in this system. First, PIPs are not anti-symmetric, that is, they are not invariant under reflection about the main diagonal and the subsequent exchange of signs. This demonstrates that selection for receptor preference is frequency-dependent (Meszéna et al. 2001). Second, evolutionary branching, the endogenous generation of two different phenotypes from a single phenotype through frequency-dependent disruptive selection (Metz et al. 1992; Geritz et al. 1998), cannot occur in this system for a wide range of plausible ecological parameters (electronic supplementary material). Third, once tradeoff strength increases to the point that perfect specialists are evolutionary end points, further increases in tradeoff strength have virtually no effect on the invasion potential of strong α2,6-specialists.

(b) ***Effects of host ecology***

We now explore how a range of relevant ecological features affect our results. First, we allow hosts to vary in their rates of contact, recovery, and loss of infectiousness. Second, we investigate a modified version of our model that might better capture the dynamics of fecal-oral and aerosol transmission between and within the reservoir and intermediate hosts. Third, we examine the effects of two possible long-term intervention strategies, changing the sizes of intermediate and target hosts and the degree of mixing between different host populations.

(i) ***Differences in host demography and epidemiology***

Natural host populations differ not only in their receptors but also in their demographic and epidemiologic rates. We therefore investigate two main features of host populations, the rate γ at which susceptible hosts are replenished and the pathogen's basic reproduction ratio R_0 in each host population.

The rate γ in equations (2*a*) and (2*c*) approximates the net effects of birth, death, immigration, emigration, and loss of immunity. We choose relatively high values of γ (1/3 and 1/6 months^{-1}, respectively) for reservoir and intermediate hosts, implying that a recovered individual will, on average, be replaced every three or six months by a susceptible host. In the intermediate hosts, such replacement mainly occurs through culling or sale. In the reservoir hosts, it occurs mainly through loss of immunity and migration. We initially assume that γ is approximately fourfold smaller (1/2 y^{-1}) in the target hosts. This choice reflects influenza's relatively fast antigenic evolution in humans, the longer lifespan of the target population, and a high rate of immigration and emigration events.

Better estimates are available for the epidemiologic rates of transmission and recovery in influenza's different host populations (table S1). A standard measure of a pathogen's fitness in a population is its basic reproduction ratio R_0, which measures the expected total number of secondary infections caused by a primary infection in an otherwise fully susceptible host population. For a perfect specialist in a population of intermediate hosts with $c = 1$, the total number of secondary cases in its own population is $R_{0,\mathrm{m}\to\mathrm{m}} = \beta_{\mathrm{mm}}/\nu_{\mathrm{m}}$. Our parameters yield R_0 values that are highest for reservoir hosts ($R_{0,\mathrm{r}\to\mathrm{r}} = 4$ for a perfect α2,3-specialist), lowest for target hosts ($R_{0,\mathrm{t}\to\mathrm{t}} = 1.5$ for a perfect α2,6-specialist), and intermediate for intermediate hosts ($R_{0,\mathrm{m}\to\mathrm{m}} = 1.75$ for either perfect specialist). These choices of R_0 and γ allow the highest disease prevalence to be reached in reservoir hosts and the highest levels of immunity in target hosts.

Changing the demography and epidemiology of the different host populations predictably breaks the symmetry in evolutionary outcomes. In general, if mixing is complete ($c = 1$) and the tradeoff is not especially weak (s larger than ≈ 0.25), perfect α2,3-specialists tend to dominate: they are the evolutionary end point from the majority of starting conditions, assuming small mutational step sizes (figures S3-S5). Even if large mutations are possible, α2,6-specialists often cannot invade perfect α2,3-specialists, or such invasion is feasible only for perfect or nearly perfect α2,6-specialists. This restriction on α2,6-specialist invasion is much more sensitive to differences in R_0 among host populations than to the rates γ of susceptible replenishment (figures S3, S4).

(ii) *Density-dependent transmission*

In wild waterfowl, influenza viruses appear to be transmitted predominantly by the fecal-oral route via contamination of shared water sources. Water is presumably also the route by which they infect domesticated animals, including pigs and chickens. Pigs and chickens generally crowd at high densities and permit aerosol transmission (electronic supplementary material). To test the robustness of our conclusions, we now assume that transmission rates under waterborne and aerosol transmission in reservoir and intermediate hosts scale more closely with the abundances than with the frequencies of infected hosts, resulting in density-dependent transmission (Keeling & Rohani 2007). In contrast, aerosol transmission involving the target hosts is better represented by frequency-dependent transmission, as transmission rates between target and intermediate hosts quickly saturate with respect to population size.

A modified version of our model thus assumes density-dependent transmission within and between reservoir and intermediate hosts, and frequency-dependent transmission within target hosts and between target and intermediate hosts. We also distinguish the amount of mixing between reservoir and intermediate hosts (c_1) from that between intermediate and target hosts (c_2). Analogous to equation (2*d*), the force of infection for the intermediate host is then

$$\lambda_{\mathrm{m}} = \max[P(\alpha 2,3), P(\alpha 2,6)]\left(\beta_{\mathrm{mr}} c_1 I_{\mathrm{r}} + \beta_{\mathrm{mm}} I_{\mathrm{m}} + \frac{\beta_{\mathrm{mt}} c_2 I_{\mathrm{t}}}{c_2 N_{\mathrm{m}} + N_{\mathrm{t}}}\right). \tag{6}$$

The shift from frequency-dependent to density-dependent transmission requires a change in the value and dimensions of β_{ij} for $i,j \in \{\mathrm{m},\mathrm{r}\}$. We choose β_{ij} so that the initial growth rates in each host are identical to the frequency-dependent case with $N_{\mathrm{r}} = N_{\mathrm{m}} = 100$ individuals. We assume that transmission is limited by the abundance of viruses in, and contact opportunities of, infecting hosts, and thus let the transmission rates equal those of the infecting host population: $\beta_{\mathrm{rm}} = \beta_{\mathrm{mm}}$ and $\beta_{\mathrm{mr}} = \beta_{\mathrm{rr}}$. For simplicity, we also assume that the transmission rate between intermediate and target hosts equals that within the target population: $\beta_{\mathrm{tt}} = \beta_{\mathrm{tm}} = \beta_{\mathrm{mt}}$. A complete description of this model version is provided by equations (S3) to (S5) (electronic supplementary material). We now explore the consequences of this varied form of transmission in the context of possible intervention strategies.

(iii) ***Sizes of intermediate and target host populations***

The abundances of the intermediate and target hosts have nonlinear effects on the ability of α2,6-specialists to invade perfect α2,3-specialists. In general, increasing the size of the intermediate host population diminishes the ability of α2,6-specialists to invade when perfect α2,3-specialists are endemic. In contrast, increasing the size of the target host population improves the ability of α2,6-adapted viruses to invade. These patterns hold for our frequency-dependent and density-dependent models, and also for neutral and non-neutral host ecologies (figures S6-S9).

There are notable quantitative differences in the evolutionary outcomes resulting from the two different transmission modes. Unsurprisingly, frequency-dependent transmission attenuates the effects of increasing abundances. In otherwise neutral host ecologies, even when the population of intermediate hosts is twice as large as the population of target hosts, invasion by α2,6-adapted viruses with a low degree of specialization is still possible when perfect α2,3-specialists are resident (figure S6*a*). Similarly, invasion by α2,6-specialists is still possible when the population of target hosts is roughly a fifth as large as those of the other hosts (figure S8). In an otherwise neutral host ecology, density-dependent transmission between reservoir and intermediate hosts also permits α2,6-invasion when intermediate host abundance is quite high (figure S6*b*). In contrast, differences in R_0 and γ among host populations greatly restrict the population sizes allowing α2,6-invasion (figures S7 and S9). For intermediate tradeoff strengths (e.g., $s = 0.75$ and $s = 1$), α2,6-specialists cannot invade and coexist if the size of target host population is lower than those of the other host populations, or if the size of intermediate host population exceeds those of the other host populations. Remarkably, the sizes of target and intermediate host populations that form the threshold for the invasion of α2,6-specialists do not change substantially as tradeoff strength varies from $s = 0.25$ to $s = 1.5$.

(iv) ***Contacts among host populations***

It is interesting to ask whether an intervention that reduces c_1 (the degree of mixing between reservoir and intermediate hosts) has a greater effect on host-range evolution than one that reduces c_2 (the degree of mixing between the intermediate and target hosts). We find that the ability of α2,6-specialists to invade and coexist with α2,3-specialists increases as transmission rates among host populations decline. This result holds when parameters c_1 and c_2 are considered under density-dependent transmission in either neutral or non-neutral host ecologies (figures S11 and S12). It also holds under frequency-dependent transmission when c_1 and c_2 are varied together (figure S10). Nonetheless, a neutral host ecology permits invasion of viruses with a low degree of α2,6-specialization even when contacts between hosts from different populations are roughly as likely as those between hosts in the same population. Under more realistic host ecologies, opportunities are much more restricted (figures S11*b* and S12*b*). For all but the weakest tradeoffs, an increase in c_1 will quickly limit the invasion potential of α2,6-adapted viruses. A greater increase in c_2 is necessary to cause the same effect.

5. DISCUSSION

We have shown how the evolution of host range, predicated on a single tradeoff, can be shaped by frequency-dependent selection, tradeoff strength, transmission mode, and host ecology. As expected, very weak tradeoffs favor generalist strategies. Unexpectedly, however, weak tradeoffs can promote the evolution and coexistence of viral phenotypes specialized on alternative receptor types, assuming large mutations are possible. In that case, both host ecology and tradeoff strength nonlinearly affect the ability of α2,6-adapted mutants to invade when α2,3-specialists are resident. The invasion of α2,6-adapted viruses is facilitated by low inter-population transmission rates, low abundances of intermediate hosts, and high abundances of target hosts (figure 3). Interestingly, these conditions are relatively insensitive to tradeoff strength. Except at extremely weak tradeoffs, epidemiological coexistence implies evolutionary coexistence; if perfect specialists cannot coexist evolutionarily, extremely well-adapted specialists can.

Tradeoff strength varies among influenza viruses. Viable intermediate phenotypes with dual receptor functionality have been reported for some subtypes but not for others. Matrosovich et al. (2001) identified a lineage of H9N2 from wild aquatic birds and poultry that retained relatively high binding affinity for both avian α2,3- and porcine α2,6-receptors. Likewise, some avian-adapted H2N2 viruses from 1957 show a weak tradeoff in binding to α2,3- and α2,6-receptors, which might have allowed them to gain a foothold in the human or pig population and then undergo further adaptations to α2,6-receptor types (Liu et al. 2009). In contrast, strains of H1N1 and H3N2 from humans and pigs often show only weak affinity for α2,3-sialosides, and exhibit a complete change in receptor preference resulting from only a few amino-acid substitutions (Matrosovich et al. 2000). Our model predicts that weak tradeoffs should allow invasion of less well adapted types (e.g., H2N2), and also that subtypes with higher tradeoff strengths would more readily give rise to the long-term coexistence of specialists. The second pattern echoes the observation that the subtypes often found circulating in pigs and humans (H1N1 and H3N2) show affinity either to α2,3- or α2,6-receptors, but not to both simultaneously.

Our results lend strong support to the idea that certain host ecologies facilitate expansions of a disease's host range. We find that, fortunately, coexistence of specialists is much more difficult in influenza's natural ecology than in a neutral one. Low inter-population transmission rates, small intermediate host populations, and large target host populations all increase the fraction of hosts that are susceptible to α2,6-mutants by limiting exposure to α2,3-viruses in the intermediate host. Low transmission rates between the intermediate and target hosts (low c_2) reduce the fraction of target hosts' contacts with intermediate hosts, some fraction of which resist infection due to previous exposure to α2,3-adapted viruses. This reduction thus opposes a potential "dilution effect" of wasting contacts on incompetent (here, immune) hosts (Schmidt & Ostfeld 2001). While the effect of increasing the population of target hosts is unsurprising, a less intuitive result is that large populations of intermediate hosts, by supporting increased exchange of α2,3-adapted viruses with the reservoir, reduce the fraction of hosts potentially susceptible to α2,6-adapted viruses. Of course, large populations of intermediate hosts in nature could pose an increased risk for the emergence of α2,6-adapted viruses if host abundance correlates positively with the pathogen's genetic diversity. This result nonetheless underscores the major roles of immunity in the intermediate host population and of the rates of contact between target and intermediate hosts.

Investigations of the system's nonequilibrium dynamics could be useful. Influenza outbreaks are seasonal in most animals, and transmission rates are likely to be seasonal. If the amplitude of epidemic oscillations is sufficiently high, equilibria of viral evolution can be different from those predicted here (White et al. 2006). Adaptation is also fundamentally probabilistic. Although we established a threshold for invasion based on positive growth of a mutant when rare, negative growth rates in nature may stochastically generate chains of mutations and transmission that are long enough to allow significant adaptation and ultimately positive growth (Andre & Day 2005; Antia et al. 2003). In other words, it may be possible for α2,6-adapted viruses to gain a foothold outside the areas of positive growth in the analyses presented here.

Increasing detail on receptor specificity in different viruses will help address questions of evolutionary attainability. The tradeoff between α2,3- and α2,6-preference provides a rough approximation of patterns in relative binding ability (Gambaryan et al. 2005). Receptor binding ability is only one small, though critical, determinant of a disease's host range (Baigent & McCauley 2003). It might be feasible to model additional adaptations indirectly as a change in tradeoff strength, which we might expect to diminish over time as compensatory mutations arise at the receptor-binding site and in other genes.

This work shows that the evolution of host range may be as sensitive to ecological considerations as it is to the physiological details of adaptation. The long-term diversity of influenza viruses, for all realistic tradeoffs, is highly sensitive to transmission rates and population sizes. Naturally or artificially acquired immunity in intermediate hosts and the dilution of contacts among competent hosts are key to reducing the long-term ability of α2,6-adapted viruses to persist.

Acknowledgements

We thank two anonymous reviewers, as well as Andrew Dobson, Casey Schneider-Mizell, Katia Koelle, and Åke Brännström for useful comments. S.C. was funded by the U.S. National Committee for IIASA, the Rackham Graduate Student Research Grant, and a NSF Graduate Research Fellowship. This work was begun while S.C. participated in the Young Scientists Summer Program at IIASA. M.P. received support from the James S. McDonnell Foundation through a Centennial Fellowship. M.P. is an investigator of the Howard Hughes Medical Institute. U.D. gratefully acknowledges support by the European Commission, the European Science Foundation, the Austrian Science Fund, the Austrian Ministry of Science and Research, and the Vienna Science and Technology Fund.

References

Andre, J. B. & Day, T. 2005 The effect of disease life history on the evolutionary emergence of novel pathogens. *Proceedings of the Royal Society B-Biological Sciences* **272**, 1949-1956.

Antia, R., Regoes, R. R., Koella, J. C. & Bergstrom, C. T. 2003 The role of evolution in the emergence of infectious diseases. *Nature* **426**, 658-661.

Baigent, S. J. & McCauley, J. W. 2003 Influenza type A in humans, mammals and birds: determinants of virus virulence, host-range and interspecies transmission. *Bioessays* **25**, 657-671.

Baranowski, E., Ruiz-Jarabo, C. M. & Domingo, E. 2001 Evolution of cell recognition by viruses. *Science* **292**, 1102-1105.

Bulaga, L. L., Garber, L., Senne, D. A., Myers, T. J., Good, R., Wainwright, S., Trock, S. & Suarez, D. L. 2003 Epidemiologic and surveillance studies on avian influenza in live-bird markets in New York and New Jersey, 2001. *Avian Diseases* **47**, 996-1001.

Dieckmann, U. & Law, R. 1996 The dynamical theory of coevolution: A derivation from stochastic ecological processes. *Journal of Mathematical Biology* **34**, 579-612.

Dieckmann, U., Metz, J. A. J., Sabelis, M. W. & Sigmund, K. 2002 *Adaptive Dynamics of Infectious Diseases: In Pursuit of Virulence Management*. Cambridge Studies in Adaptive Dynamics. Cambridge, U.K.: Cambridge University Press.

Egas, M., Dieckmann, U. & Sabelis, M. W. 2004 Evolution restricts the coexistence of specialists and generalists: The role of trade-off structure. *American Naturalist* **163**, 518-531.

Gambaryan, A., Yamnikova, S., Lvov, D., Tuzikov, A., Chinarev, A., Pazynina, G., Webster, R., Matrosovich, M. & Bovin, N. 2005 Receptor specificity of influenza viruses from birds and mammals: New data on involvement of the inner fragments of the carbohydrate chain. *Virology* **334**, 276-283.

Gambaryan, A. S., Yamnikova, S. S., Lvov, D. K., Robertson, J. S., Webster, R. G. & Matrosovich, M. N. 2002 Differences in receptor specificity between the influenza viruses of duck, chicken, and human. *Molecular Biology* **36**, 429-435.

Gandon, S. 2004 Evolution of multihost parasites. *Evolution* **58**, 455-469.

Geritz, S. A. H., Kisdi, É., Meszéna, G. & Metz, J. A. J. 1998 Evolutionarily singular strategies and the adaptive growth and branching of the evolutionary tree. *Evolutionary Ecology* **12**, 35-57.

Ito, T., Kawaoka, Y., Nomura, A. & Otsuki, K. 1999 Receptor specificity of influenza A viruses from sea mammals correlates with lung sialyloligosaccharides in these animals. *Journal of Veterinary Medical Science* **61**, 955-958.

Keeling, M. J. & Rohani, P. 2007 *Modeling Infectious Diseases in Humans and Animals*. Princeton, NJ: Princeton University Press.

Kida, H., Ito, T., Yasuda, J., Shimizu, Y., Itakura, C., Shortridge, K. F., Kawaoka, Y. & Webster, R. G. 1994 Potential for transmission of avian influenza-viruses to pigs. *Journal of General Virology* **75**, 2183-2188.

Koelle, K., Pascual, M. & Yunus, M. 2005 Pathogen adaptation to seasonal forcing and climate change. *Proceedings of the Royal Society of London, Series B-Biological Sciences* **272**, 971-977.

Levins, R. 1962 Theory of fitness in a heterogeneous environment. I. The fitness set and adaptive function. *The American Naturalist* **96**, 361-373.

Liu, J. F., Stevens, D. J., Haire, L. F., Walker, P. A., Coombs, P. J., Russell, R. J., Gamblin, S. J. & Skehel, J. J. 2009 Structures of receptor complexes formed by hemagglutinins from the Asian Influenza pandemic of 1957. *Proceedings of the National Academy of Sciences of the United States of America* **106**, 17175-17180.

Liu, M., He, S. Q., Walker, D., Zhou, N. N., Perez, D. R., Mo, B., Li, F., Huang, X. T., Webster, R. G. & Webby, R. J. 2003 The influenza virus gene pool in a poultry market in South Central China. *Virology* **305**, 267-275.

Matrosovich, M., Tuzikov, A., Bovin, N., Gambaryan, A., Klimov, A., Castrucci, M. R., Donatelli, I. & Kawaoka, Y. 2000 Early alterations of the receptor-binding properties of H1, H2, and H3 avian influenza virus hemagglutinins after their introduction into mammals. *Journal of Virology* **74**, 8502-8512.

Matrosovich, M. N., Krauss, S. & Webster, R. G. 2001 H9N2 influenza A viruses from poultry in Asia have human virus-like receptor specificity. *Virology* **281**, 156-162.

Meszéna, G., Kisdi, É., Dieckmann, U., Geritz, S. A. H. & Metz, J. A. J. 2001 Evolutionary optimization models and matrix games in the unified perspective of adaptive dynamics. *Selection 2* **2**, 193-210.

Metz, J. A. J., Geritz, S. A. H., Meszéna, G., Jacobs, F. J. A. & van Heerwaarden, J. S. 1996 Adaptive dynamics: a geometrical study of the consequences of nearly faithful reproduction. In *Stochastic and Spatial Structures of Dynamical Systems* (ed. S. J. van Strien & S. M. Verduyn Lunel), pp. 183-231. Amsterdam: North Holland.

Metz, J. A. J., Nisbet, R. M. & Geritz, S. A. H. 1992 How should we define fitness for general ecological scenarios? *Trends in Ecology & Evolution* **7**, 198-202.

Parker, G. A., Chubb, J. C., Ball, M. A. & Roberts, G. N. 2003 Evolution of complex life cycles in helminth parasites. *Nature* **425**, 480-484.

Schmidt, K. A. & Ostfeld, R. S. 2001 Biodiversity and the dilution effect in disease ecology. *Ecology* **82**, 609-619.

Scholtissek, C., Hinshaw, V. S. & Olsen, C. W. 1998 Influenza in pigs and their role as the intermediate host. In *Textbook of Influenza* (ed. K. G. Nicholson, R. G. Webster & A. J. Hay), pp. 137-145. Malden, MA: Blackwell Science.

Webby, R., Hoffmann, E. & Webster, R. 2004 Molecular constraints to interspecies transmission of viral pathogens. *Nature Medicine* **10**, S77-S81.

Webster, R. G. 2004 Wet markets - a continuing source of severe acute respiratory syndrome and influenza? *Lancet* **363**, 234-236.

Webster, R. G., Bean, W. J., Gorman, O. T., Chambers, T. M. & Kawaoka, Y. 1992 Evolution and Ecology of Influenza-A Viruses. *Microbiological Reviews* **56**, 152-179.

Webster, R. G. & Hulse, D. J. 2004 Microbial adaptation and change: avian influenza. *Revue Scientifique et Technique de l'Office International des Epizooties* **23**, 453-465.

White, A., Greenman, J. V., Benton, T. G. & Boots, M. 2006 Evolutionary behaviour in ecological systems with trade-offs and non-equilibrium population dynamics. *Evolutionary Ecology Research*, 387-398.

Woolhouse, M. E. J. & Gowtage-Sequeria, S. 2005 Host range and emerging and reemerging pathogens. *Emerging Infectious Diseases* **11**, 1842-1847.

Figure captions

Figure 1. (*a*) Transmission structure of host community, highlighting receptor conformations in three host populations: reservoir hosts (waterfowl; r), intermediate hosts (pigs and chickens; m), and target hosts (humans; t). Population sizes in each class are denoted by N_i with i = r, m, t. (*b*) Tradeoff for receptor preference. The strength of the tradeoff is given by s, with $s < 1$ characterizing a weak tradeoff and $s > 1$ a strong tradeoff. Moving away from the origin, the curves correspond to s = 1.5, 1, 0.75, 0.5, 0.25, and 0.05. Colors indicate the degree of specialization on the nearby receptor: red (high specialization), orange (low specialization), and blue (negligible specialization: generalists).

Figure 2. Evolutionary outcomes in a neutral host ecology. (*a*) Pairwise invasibility plots for different tradeoff strengths s for $N_\mathrm{t} = N_\mathrm{m} = N_\mathrm{r}$, $c = 1$, $\beta_\mathrm{rr} = \beta_\mathrm{mm} = \beta_\mathrm{tt} = 1/3$ days^{-1}, $\nu_\mathrm{r} = \nu_\mathrm{m} = \nu_\mathrm{t} = 1/6$ days^{-1}, and $\gamma_\mathrm{r} = \gamma_\mathrm{m} = \gamma_\mathrm{t} = 1/180$ days^{-1}. Black (white) areas indicate where the mutant has a positive (negative) growth rate in the endemic environment determined by the resident. Gray areas indicate regions in which the resident phenotype is not viable. (*b*) Trait evolution plots for the pairwise invasibility plots in (*a*). Gray areas indicate phenotype pairs that are mutually invasible and that therefore can coexist and coevolve. Black lines are evolutionary isoclines at which the selection pressure on one phenotype vanishes. Circles correspond to evolutionary attractors if filled and to evolutionary repellors if open. Arrows show the directions, at the quadrant level, of positive selection pressures (for better readability, such arrows are shown here only for the largest bounded regions).

Figure 3. Conditions that permit the coexistence of perfect specialists, assuming frequency-dependent transmission, realistic ecological parameters of host populations (table S1), and a linear tradeoff (s =1). Parameter combinations that permit specialist coexistence are in gray. Coexistence is evolutionarily stable for higher tradeoffs (s = 0.75 and above), but not for weaker tradeoffs; however, even at weaker tradeoffs, extremely well adapted viruses are able to coexist (see text, fig. 2). (*a*) Effects of the relative population size $N_m/N_r = N_m/N_t$ of intermediate hosts and of the degree c_1 of mixing between reservoir and intermediate hosts. (*b*) Effects of the relative population size $N_t/N_r = N_t/N_m$ of target hosts and of the degree c_2 of mixing between intermediate and target hosts.

Short title for page headings: Evolution of influenza’s host range

Figure 1

(*a*)

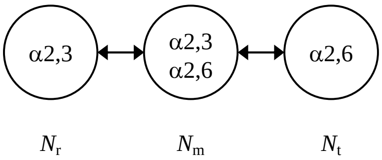
α2,3
α2,3
α2,6
α2,6
N_r
N_m
N_t

(*b*)

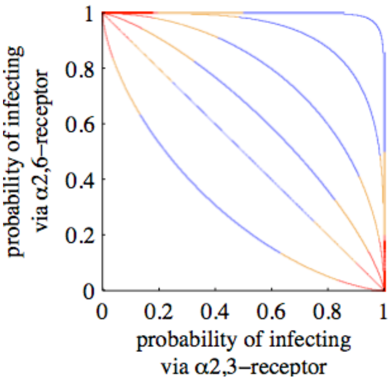
1
0.8
0.6
0.4
0.2
0
0
0.2
0.4
0.6
0.8
1
probability of infecting via α2,6–receptor
probability of infecting via α2,3–receptor

Figure 2

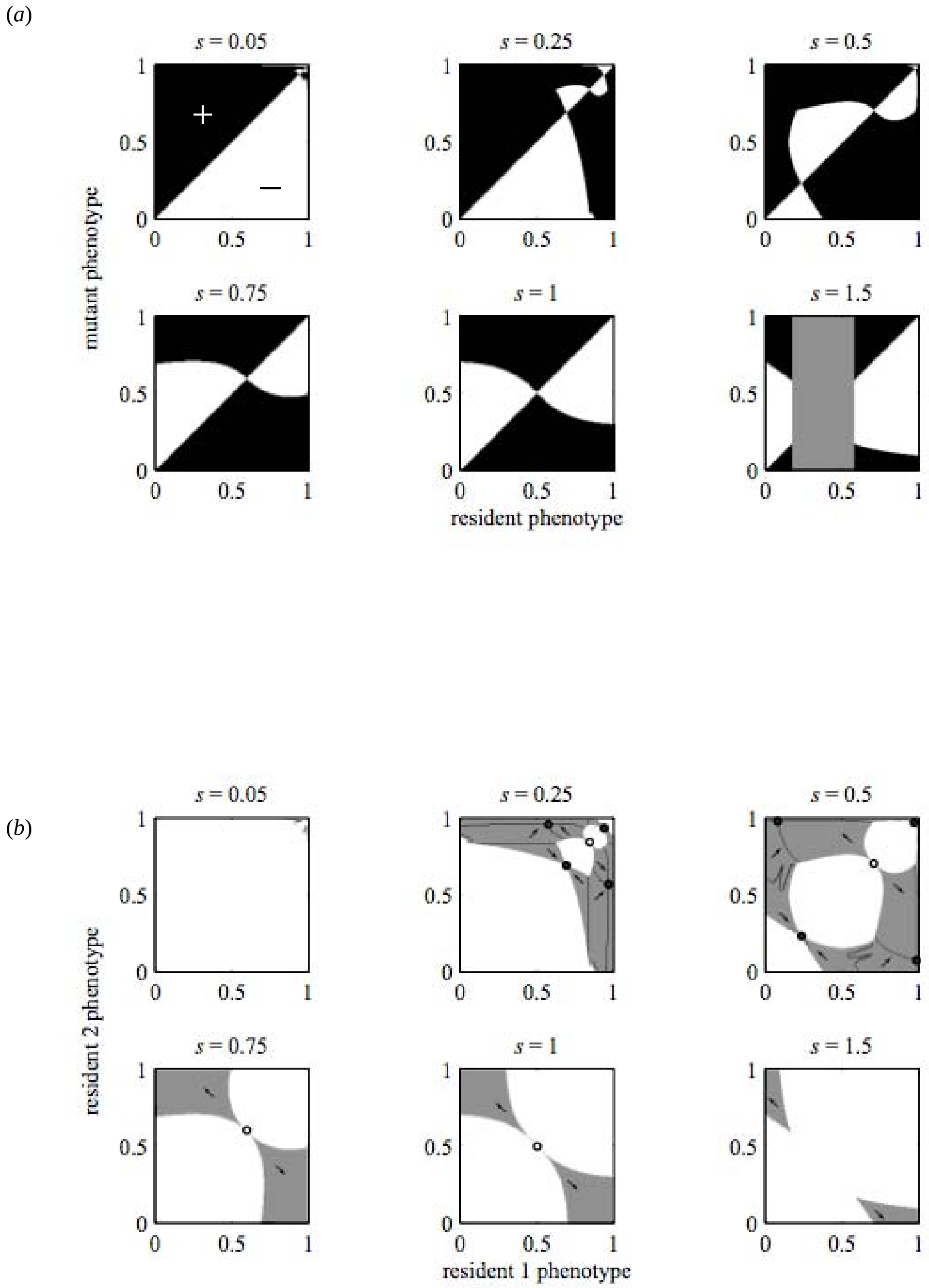
(a)
s = 0.05
s = 0.25
s = 0.5
s = 0.75
s = 1
s = 1.5
+
–
mutant phenotype
resident phenotype
0
0.5
1
(b)
s = 0.05
s = 0.25
s = 0.5
s = 0.75
s = 1
s = 1.5
resident 2 phenotype
resident 1 phenotype
0
0.5
1

Figure 3

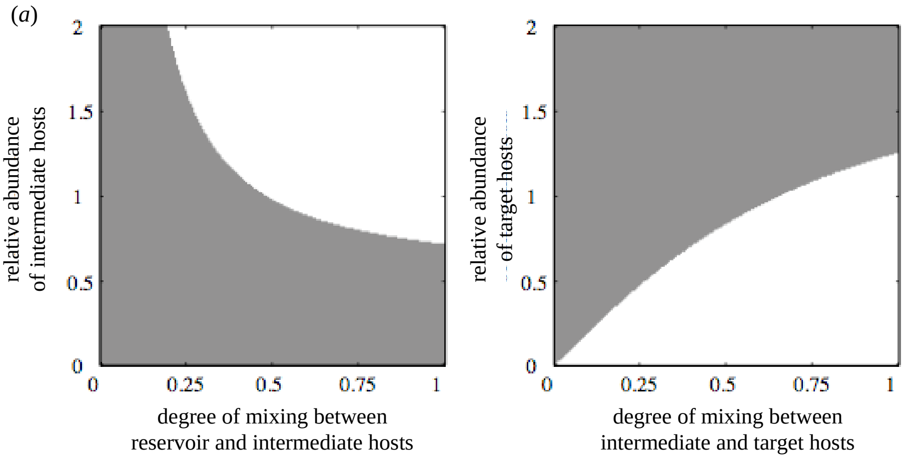
(a)
relative abundance of intermediate hosts
2
1.5
1
0.5
0
0
0.25
0.5
0.75
1
degree of mixing between reservoir and intermediate hosts
relative abundance of target hosts
2
1.5
1
0.5
0
0
0.25
0.5
0.75
1
degree of mixing between intermediate and target hosts

Electronic Supplementary Material

for

Ecological factors driving the long-term evolution of influenza’s host range

Sarah Cobey, Mercedes Pascual, and Ulf Dieckmann

Contents

I. Equations for intermediate and target hosts for model with frequency-dependent transmission
II. The Jacobian of the model with frequency-dependent transmission
III. Default parameters (table S1)
IV. Equations for model with density-dependent transmission
V. Figures
    a. Captions
    b. Effects of tradeoff strength in a neutral ecology
        i. Figure S1 (R_0 = 1.5)
        ii. Figure S2 (R_0 = 4)
    c. Effects of host ecology
        i. Differences in host demography and epidemiology
            1. Figure S3 (c = 1, R_0 constant, varying γ)
            2. Figure S4 (c = 1, varying R_0, constant γ)
            3. Figure S5 (c = 1, varying both R_0 and γ)
        ii. Intermediate and target host population sizes
            1. Figure S6 (varying N_m in a neutral ecology)
            2. Figure S7 (varying N_m in a non-neutral ecology)
            3. Figure S8 (varying N_t in a neutral ecology)
            4. Figure S9 (varying N_t in a non-neutral ecology)
        iii. Relative rates of interspecific transmission
            1. Figure S10: Varying c_1 (reservoir-intermediate host) and c_2 (target-intermediate host) identically when all transmission is frequency-dependent
            2. Figure S11: Varying c_1 only with density dependence
            3. Figure S12: Varying c_2 only with density dependence
VI. References

I. Equations for intermediate and target hosts for model with frequency-dependent transmission

SIRS equations for the population of intermediate hosts are given in the main text (eqs. 2a-c). The corresponding SIRS equations for the population of reservoir hosts are

$$\frac{\mathrm{d}S_{\mathrm{r}}}{\mathrm{d}t}=\gamma_{\mathrm{r}}R_{\mathrm{r}}-P(\alpha 2,3)\left(\frac{\beta_{\mathrm{rr}}I_{\mathrm{r}}}{N_{\mathrm{r}}+cN_{\mathrm{m}}}+\frac{\beta_{\mathrm{rm}}cI_{\mathrm{m}}}{cN_{\mathrm{r}}+N_{\mathrm{m}}+cN_{\mathrm{t}}}\right)S_{\mathrm{r}}\ , \tag{S1a}$$

$$\frac{\mathrm{d}I_{\mathrm{r}}}{\mathrm{d}t}=P(\alpha 2,3)\left(\frac{\beta_{\mathrm{rr}}I_{\mathrm{r}}}{N_{\mathrm{r}}+cN_{\mathrm{m}}}+\frac{\beta_{\mathrm{rm}}cI_{\mathrm{m}}}{cN_{\mathrm{r}}+N_{\mathrm{m}}+cN_{\mathrm{t}}}\right)S_{\mathrm{r}}-\nu_{\mathrm{r}}I_{\mathrm{r}}\ , \tag{S1b}$$

$$\frac{\mathrm{d}R_{\mathrm{r}}}{\mathrm{d}t}=\nu_{\mathrm{r}}I_{\mathrm{r}}-\gamma_{\mathrm{r}}R_{\mathrm{r}}\ . \tag{S1c}$$

Analogously, SIRS equations for the population of target hosts are

$$\frac{\mathrm{d}S_{\mathrm{t}}}{\mathrm{d}t}=\gamma_{\mathrm{t}}R_{\mathrm{t}}-P(\alpha 2,6)\left(\frac{\beta_{\mathrm{tt}}I_{\mathrm{t}}}{N\mathrm{t}+cN_{\mathrm{m}}}+\frac{\beta_{\mathrm{tm}}cI_{\mathrm{m}}}{cN_{\mathrm{r}}+N_{\mathrm{m}}+cN_{\mathrm{t}}}\right)S_{\mathrm{t}}\ , \tag{S2a}$$

$$\frac{\mathrm{d}I_{\mathrm{t}}}{\mathrm{d}t}=P(\alpha 2,6)\left(\frac{\beta_{\mathrm{tt}}I_{\mathrm{t}}}{N_{\mathrm{t}}+cN_{\mathrm{m}}}+\frac{\beta_{\mathrm{tm}}cI_{\mathrm{m}}}{cN_{\mathrm{r}}+N_{\mathrm{m}}+cN_{\mathrm{t}}}\right)S_{\mathrm{t}}-\nu_{\mathrm{t}}I_{\mathrm{t}}\ , \tag{S2b}$$

$$\frac{\mathrm{d}R_{\mathrm{t}}}{\mathrm{d}t}=\nu_{\mathrm{t}}I_{\mathrm{t}}-\gamma_{\mathrm{t}}R_{\mathrm{t}}\ . \tag{S2c}$$

II. The Jacobian of the model with frequency-dependent transmission

The Jacobian matrix of a rare mutant's epidemiological dynamics is given by

$$J = \begin{bmatrix} P_1(\alpha 2,3)\left(\frac{\beta_{\mathrm{rr}} S_{\mathrm{r}}^*}{N_{\mathrm{r}} + cN_{\mathrm{m}}}\right) - \nu_{\mathrm{r}} & P_1(\alpha 2,3)\left(\frac{\beta_{\mathrm{rm}} c S_{\mathrm{r}}^*}{cN_{\mathrm{r}} + N_{\mathrm{m}} + cN_{\mathrm{t}}}\right) & 0 \\ \max[P_1(\alpha 2,3), P_1(\alpha 2,6)]\left(\frac{\beta_{\mathrm{mr}} c S_{\mathrm{m}}^*}{N_{\mathrm{r}} + cN_{\mathrm{m}}}\right) & \max[P_1(\alpha 2,3), P_1(\alpha 2,6)]\left(\frac{\beta_{\mathrm{mm}} S_{\mathrm{m}}^*}{cN_{\mathrm{r}} + N_{\mathrm{m}} + cN_{\mathrm{t}}}\right) - \nu_{\mathrm{m}} & \max[P_1(\alpha 2,3), P_1(\alpha 2,6)]\left(\frac{\beta_{\mathrm{mt}} c S_{\mathrm{m}}^*}{cN_{\mathrm{m}} + N_{\mathrm{t}}}\right) \\ 0 & P_1(\alpha 2,6)\left(\frac{\beta_{\mathrm{mm}} c S_{\mathrm{t}}^*}{cN_{\mathrm{r}} + N_{\mathrm{m}} + cN_{\mathrm{t}}}\right) & P_1(\alpha 2,6)\left(\frac{\beta_{\mathrm{mt}} S_{\mathrm{t}}^*}{cN_{\mathrm{m}} + N_{\mathrm{t}}}\right) - \nu_{\mathrm{t}} \end{bmatrix}$$

P_1 refers to the phenotype of the rare mutant virus. The elements J_{ij} are the instantaneous per capita rates of mutant infections spreading from infected hosts in population *j* to susceptible hosts in population *i*. Host abundances at the endemic equilibrium of the resident virus are denoted by an asterisk.

III. Default parameters

We choose parameters in keeping with general observations on the relative growth rates of different influenza subtypes in different hosts (Webster et al. 1992) (Table S1):

- The rates of loss of immunity, γ_i, are qualitative estimates based on several observations. Rates are highest in waterfowl, since they appear to have little long-term immunity to influenza. The intermediate hosts, as domesticated animals, also have relatively high turnover. Turnover rates in the target population are low due to longer host lifespans and long-lasting immunity (whose loss of immunity is here a proxy for antigenic evolution). However, we assume they are offset by relatively high host mobility (migration).

- The assumption of frequent, regular contact (suitable for transmission) between intermediate hosts and target hosts such as humans, in both rural and more industrial settings, is supported by serological surveys of pigs (Brown et al. 1995; Olsen et al. 2000; Yu et al. 2007) and by observations on asymptomatic pig-farm workers (Campitelli et al. 1997; Halvorson et al. 1983; Karunakaran et al. 1983; Myers et al. 2006; Olsen et al. 2002; Sivanandan et al. 1991) and poultry workers (Koopmans et al. 2004).

Motivation for density-dependent transmission between the reservoir and intermediate host populations comes from Brown et al. (2000), Ly et al. (2007), and Alexander (2000).

Table S1. Default parameter values used in non-neutral models. Note that "individuals" in the denominator of β_{rr} and β_{mm} in the model with density-dependent transmission is a pseudo-unit.

Symbol	**Description**	**Value**	**References**
ν_r	Rate of recovery in reservoir hosts	1/(12 days)	Hulse-Post et al. (2005)
ν_m	Rate of recovery in intermediate hosts	1/(7 days)	Hinshaw et al. (1981), Brown (2000); Van der Goot et al. (2003)
ν_t	Rate of recovery in target hosts	1/(6 days)	Leekha et al. (2007); Carrat et al. (2008)
γ_r	Rate of susceptible replenishment in reservoir hosts	1/(90 days)	Kida et al. (1980); Hulse-Post et al. (2005)
γ_m	Rate of susceptible replenishment in intermediate hosts	1/(180 days)	
γ_t	Rate of susceptible replenishment in target hosts	1/(730 days)	
c (c_1, c_2)	Expected probability that a member of one host population can contact another host population (for reservoir and intermediate hosts, for intermediate and target hosts)	1.0 (except where explicitly varied)	
β_{tt}	Transmission rate among target hosts	1/(4 days)	Saenz et al. (2006)
Model with frequency-dependent transmission			
β_{rr}	Transmission rate among reservoir hosts	1/(3 days)	
β_{mm}	Transmission rate among intermediate hosts	1/(4 days)	Saenz et al. (2006)
Model with density-dependent transmission			
β_{rr}	Transmission rate among reservoir hosts	1/(300 days · individuals)	
β_{mm}	Transmission rate among intermediate hosts	1/(400 days · individuals)	Saenz et al. (2006)

IV. Equations for model with density-dependent transmission

All parameters and variables are as defined in the main text.

Reservoir, r

$$\frac{dS_r}{dt} = \gamma_r R_r - P(\alpha 2,3) S_r \left(\beta_{rr} I_r + \beta_{rm} c_1 I_m\right) \tag{S3a}$$

$$\frac{dI_r}{dt} = P(\alpha 2,3) S_r \left(\beta_{rr} I_r + \beta_{rm} c_1 I_m\right) - \nu_r I_r \tag{S3b}$$

$$\frac{dR_r}{dt} = \nu_r I_r - \gamma_r R_r \tag{S3c}$$

Intermediate host, m

$$\frac{dS_m}{dt} = \gamma_m R_m - \max[P(\alpha 2,3), P(\alpha 2,6)] S_m \left(\beta_{mr} c_1 I_r + \beta_{mm} I_m + \frac{\beta_{mt} c_2 I_t}{c_2 N_m + N_t}\right) \tag{S4a}$$

$$\frac{dI_m}{dt} = \max[P(\alpha 2,3), P(\alpha 2,6)] S_m \left(\beta_{mr} c_1 I_r + \beta_{mm} I_m + \frac{\beta_{mt} c_2 I_t}{c_2 N_m + N_t}\right) - \nu_m I_m \tag{S4b}$$

$$\frac{dR_m}{dt} = \nu_m I_m - \gamma_m R_m \tag{S4c}$$

Target host, t

$$\frac{dS_t}{dt} = \gamma_t R_t - P(\alpha 2,6) S_t \left(\frac{\beta_{tm} c_2 I_m}{c_2 N_t + N_m} + \frac{\beta_{tt} I_t}{N_t + c_2 N_m}\right) \tag{S5a}$$

$$\frac{dI_t}{dt} = P(\alpha 2,6) S_t \left(\frac{\beta_{tm} c_2 I_m}{c_2 N_t + N_m} + \frac{\beta_{tt} I_t}{N_t + c_2 N_m}\right) - \nu_t I_t \tag{S5b}$$

$$\frac{dR_t}{dt} = \nu_t I_t - \gamma_t R_t \tag{S5c}$$

V. Figures

Figure S1. Pairwise invasibility (*a*) and trait evolution (*b*) plots for hosts that are identical except for their receptor preferences. Parameters are identical to figure 2, except $\nu_\mathrm{r} = \nu_\mathrm{m} = \nu_\mathrm{t} = 1/4.5$ days^{-1} (and thus intraspecific R_0 for the appropriate specialist in each species is 1.5). Gray areas in (*a*) indicate regions where the resident is inviable, whereas in (*b*) they denote regions of coexistence. In the trait evolution plots, black lines are isoclines and black circles correspond to evolutionary attractors if filled and repellors if open. Arrows show the direction at the quadrant level of selection pressure. For clarity, they are sometimes shown extending outside the plot, though phenotypes are bounded by the axes.

Figure S2. Pairwise invasibility (*a*) and trait evolution (*b*) plots for hosts that are identical except for their receptor preferences. Parameters are identical to figure 2, except $\nu_\mathrm{r} = \nu_\mathrm{m} = \nu_\mathrm{t} = 1/12$ days^{-1} (and thus R_0 for the appropriate specialist in each species is 4). Gray areas in (*b*) denote regions of coexistence. In the trait evolution plots, black lines are isoclines and black circles correspond to evolutionary attractors if filled and repellors if open. Arrows show the direction at the quadrant level of selection pressure. For clarity, they are sometimes shown extending outside the plot, though phenotypes are bounded by the axes.

Figure S3. Pairwise invasibility (*a*, *c*) and trait evolution (*b*, *d*) plots for host populations differing in their rates of susceptible replenishment γ but not R_0. In all plots, γ_r = 1/90 days^{-1} and γ_m = 1/180 days^{-1}. The intraspecific R_0 for all hosts is 2 ($\beta_{rr} = \beta_{mm} = \beta_{tt}$ = 1/3 days^{-1}, $\nu_r = \nu_m = \nu_t$ = 1/6 days^{-1}). Hosts have equal population sizes, populations mix freely (c = 1), and transmission rates are frequency-dependent. In (*a*) and (*b*), γ_t = 1/730 days^{-1}. In (*c*) and (*d*), γ_t = 1/7300 days^{-1}. Gray areas in (*a*) indicate regions where the resident is inviable, whereas in (*b*) they denote regions of coexistence. In the trait evolution plots, black lines are evolutionary isoclines and black circles correspond to evolutionary attractors if filled and repellors if open. Arrows show the direction at the quadrant level of selection pressure. For clarity, they are sometimes shown extending outside the plot, though phenotypes are bounded by the axes.

Figure S4. Pairwise invasibility (*a*) and trait evolution (*b*) plots for host populations differing in their R_0 but not their rate of susceptible replenishment. Here, intraspecific R_0 is 4 in the reservoir (β_{rr} = 1/3 days^{-1}, ν_r = 1/12 days^{-1}), 1.75 in the intermediate host (β_{mm} = 1/4 days^{-1}, ν_m = 1/7 days^{-1}), and 1.5 in the target host (β_{tt} = 1/4 days^{-1}, ν_t = 1/6 days^{-1}), as in table S1. Hosts have identical population sizes and rates of susceptible replenishment ($\gamma_r = \gamma_m = \gamma_t$ = 1/180 days^{-1}), populations mix freely (c = 1), and transmission rates are frequency-dependent. Gray areas in (*a*) indicate regions where the resident is inviable, whereas in (*b*) they denote regions of coexistence. In the trait evolution plots, black lines are evolutionary isoclines and black circles correspond to evolutionary attractors if filled and repellors if open. Arrows show the direction at the quadrant level of selection pressure.

Figure S5. Pairwise invasibility (*a*, *c*) and trait evolution (*b*, *d*) plots allowing both intraspecific R_0 and rates of susceptible replenishment to vary among hosts. Parameters are the same as those used for figure S4, except where noted, and rates of susceptible replenishment are the same ones used for figure S3 and listed in table S1. For (*c*) and (*d*), intraspecific R_0 in the reservoir ($R_0 = 2$; $\nu_r = 1/6$ days^{-1}) is lower than in (*a*) and (*b*), though in both cases it is still higher than in the intermediate ($R_0 = 1.75$) and target hosts ($R_0 = 1.5$). Gray areas in (*a*) indicate regions where the resident is inviable, whereas in (*b*) they denote regions of coexistence. In the trait evolution plots, black lines are evolutionary isoclines and black circles correspond to evolutionary attractors if filled and repellors if open. Arrows show the direction at the quadrant level of selection pressure.

Figure S6. Coexistence plots showing the effects of changing intermediate host abundance in a neutral ecology, assuming (*a*) frequency-dependent and (*b*) density-dependent transmission. Ecological parameters are the same as those used in figure 2 (for all hosts, $R_0 = 2$ and $\gamma = 1/180$ days^{-1}). Pairwise invasibility and trait evolution plots corresponding to where $N_m = N_t = N_r$ with frequency-dependent transmission are shown in figure 2. Plus signs indicate areas of coexistence, which correspond to the gray regions of trait evolution plots.

Figure S7. Coexistence plots showing the effects of changing intermediate host abundance in a non-neutral ecology, assuming (*a*) frequency-dependent and (*b*) density-dependent transmission. Ecological parameters are the same as those used in table S1.

Pairwise invasibility and trait evolution plots corresponding to where $N_\mathrm{m} = N_\mathrm{t} = N_\mathrm{r}$ with frequency-dependent transmission are shown in figure S5(*a*, *b*). Plus signs indicate areas of coexistence, which correspond to the gray regions of trait evolution plots.

Figure S8. Coexistence plots showing the effects of changing target host abundance in a neutral ecology, assuming frequency-dependent transmission. Ecological parameters are the same as those used in figure 2 (for all hosts, $R_0 = 2$ and $\gamma = 1/180$ days^{-1}). Pairwise invasibility and trait evolution plots corresponding to where $N_\mathrm{t} = N_\mathrm{m} = N_\mathrm{r}$ with frequency-dependent transmisison are shown in figure 2. Plus signs indicate areas of coexistence, which correspond to the gray regions of trait evolution plots.

Figure S9. Effects of changing target host abundance in a non-neutral ecology, assuming frequency-dependent transmission. Ecological parameters are the same as those used in table S1. Pairwise invasibility and trait evolution plots corresponding to where $N_\mathrm{t} = N_\mathrm{m} = N_\mathrm{r}$ with frequency-dependent transmission are shown in figure S5(*a*,*b*). Plus signs indicate areas of coexistence, which correspond to the gray regions of trait evolution plots.

Figure S10. Coexistence plots showing effects of changing the degree of mixing between populations ($c = c_1 = c_2$) when all transmission rates are frequency-dependent. Coexistence plots are shown for (*a*) neutral and (*b*) non-neutral ecologies. Pairwise invasibility and trait evolution plots corresponding to the case where $c = 1$ are shown in figure 2 and figure S5(*a*, *b*), respectively, assuming frequency-dependent transmission.

Plus signs indicate areas of coexistence, which correspond to the gray regions of trait evolution plots.

Figure S11. Coexistence plots showing effects of changing only the scaling on rates of interspecific transmission between the reservoir and intermediate host populations (c_1) in (*a*) neutral and (*b*) non-neutral ecologies, assuming density-dependent transmission between the reservoir and intermediate host populations. Plus signs indicate areas of coexistence, which correspond to the gray regions of trait evolution plots.

Figure S12. Coexistence plots showing effects of changing only the degree of mixing between the intermediate and target populations (c_2) in (*a*) neutral and (*b*) non-neutral ecologies, assuming density-dependent transmission between the reservoir and intermediate host populations. Plus signs indicate areas of coexistence, which correspond to the gray regions of trait evolution plots.

Figure S1

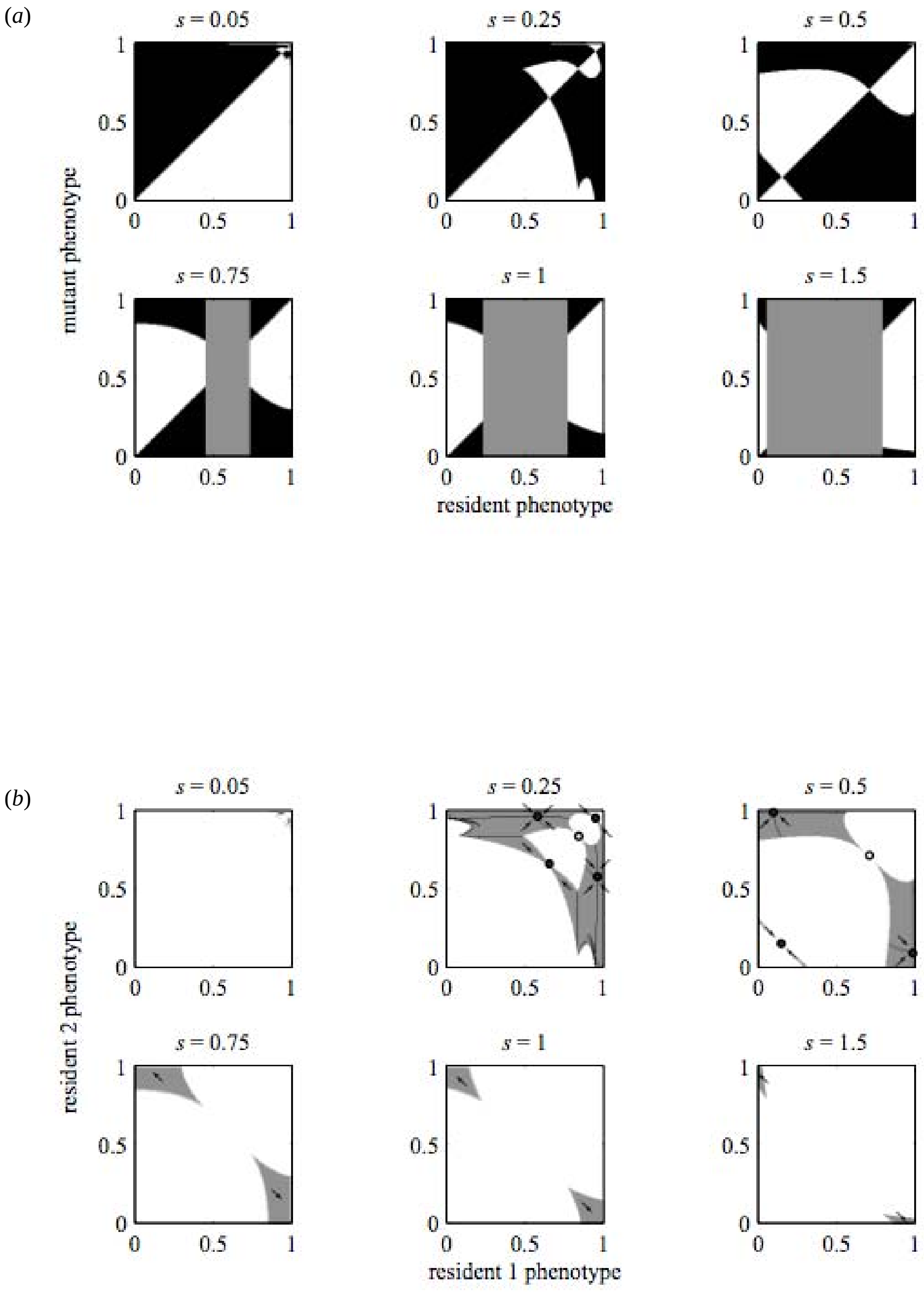
(a)
s = 0.05
s = 0.25
s = 0.5
s = 0.75
s = 1
s = 1.5
mutant phenotype
resident phenotype
0
0.5
1
(b)
s = 0.05
s = 0.25
s = 0.5
s = 0.75
s = 1
s = 1.5
resident 2 phenotype
resident 1 phenotype
0
0.5
1

Figure S2

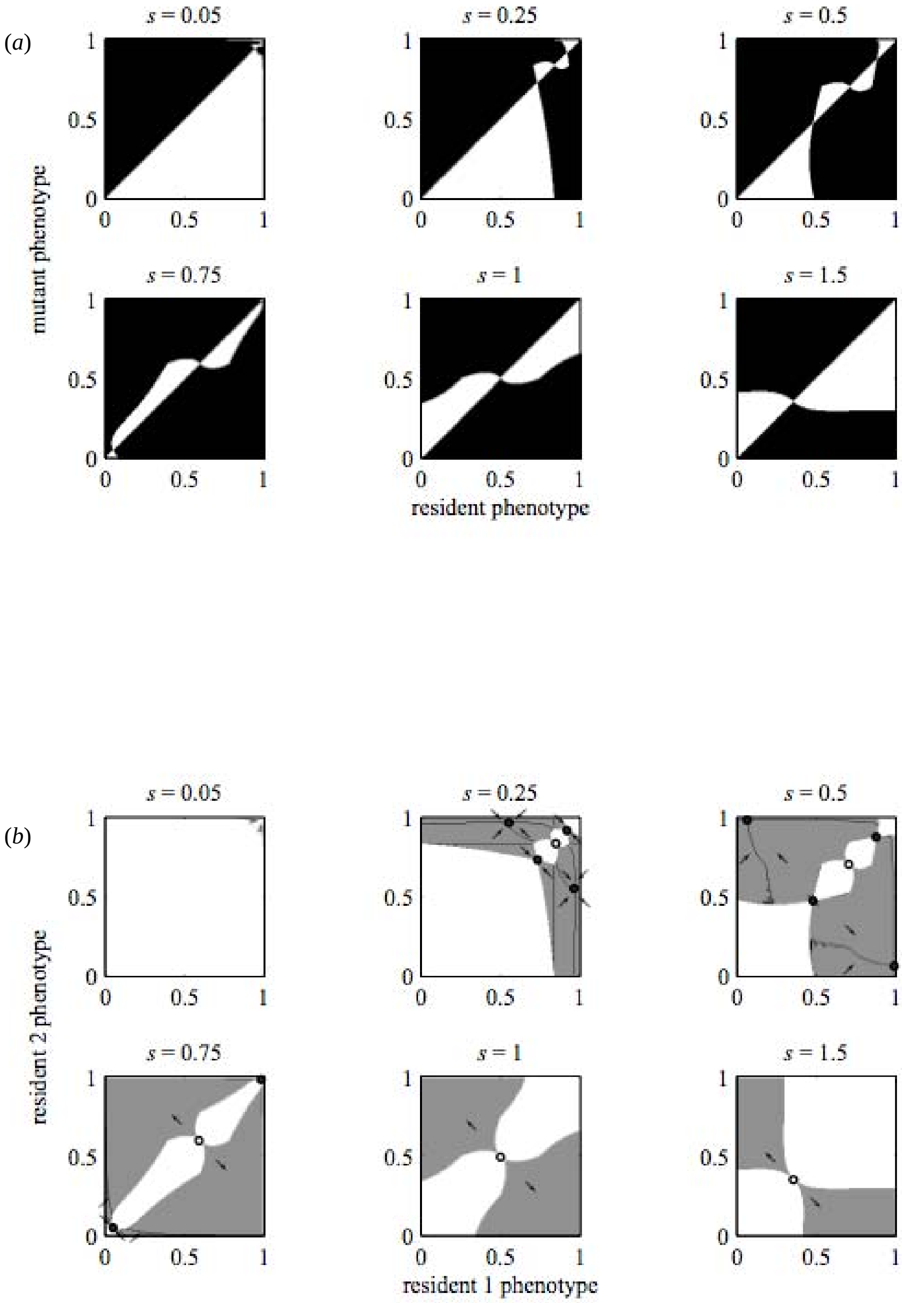
(a)
s = 0.05
s = 0.25
s = 0.5
s = 0.75
s = 1
s = 1.5
mutant phenotype
resident phenotype
0
0.5
1
(b)
s = 0.05
s = 0.25
s = 0.5
s = 0.75
s = 1
s = 1.5
resident 2 phenotype
resident 1 phenotype

Figure S3

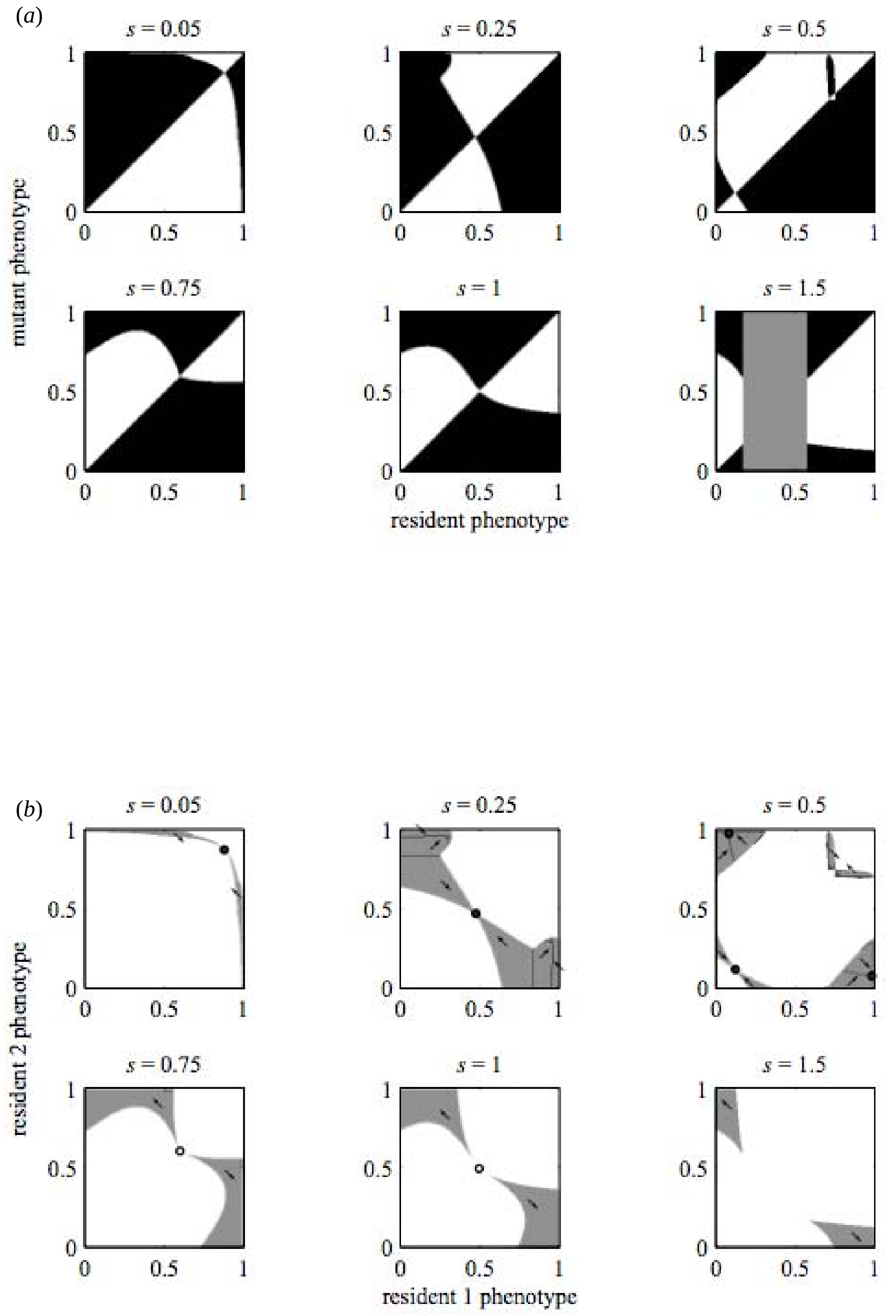
(a)
s = 0.05
s = 0.25
s = 0.5
s = 0.75
s = 1
s = 1.5
mutant phenotype
resident phenotype
0
0.5
1
(b)
s = 0.05
s = 0.25
s = 0.5
s = 0.75
s = 1
s = 1.5
resident 2 phenotype
resident 1 phenotype
0
0.5
1

Figure S3 (continued)

(*c*)

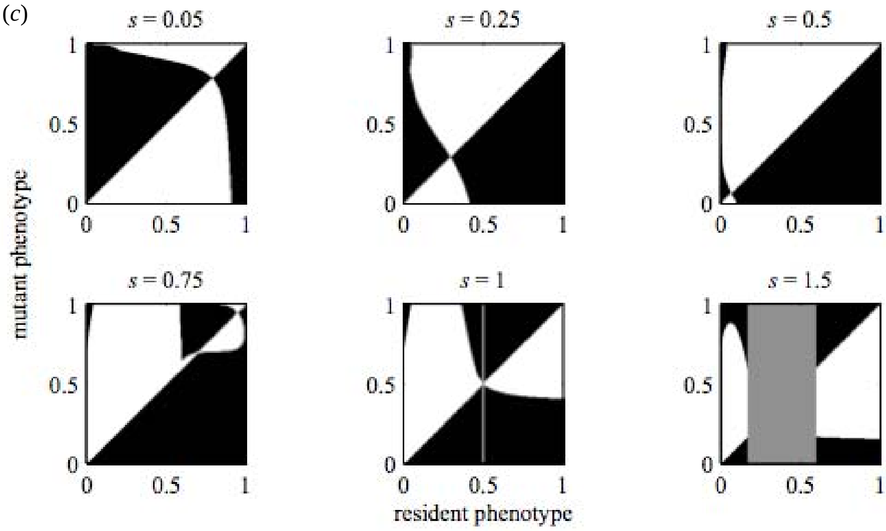

(*d*)

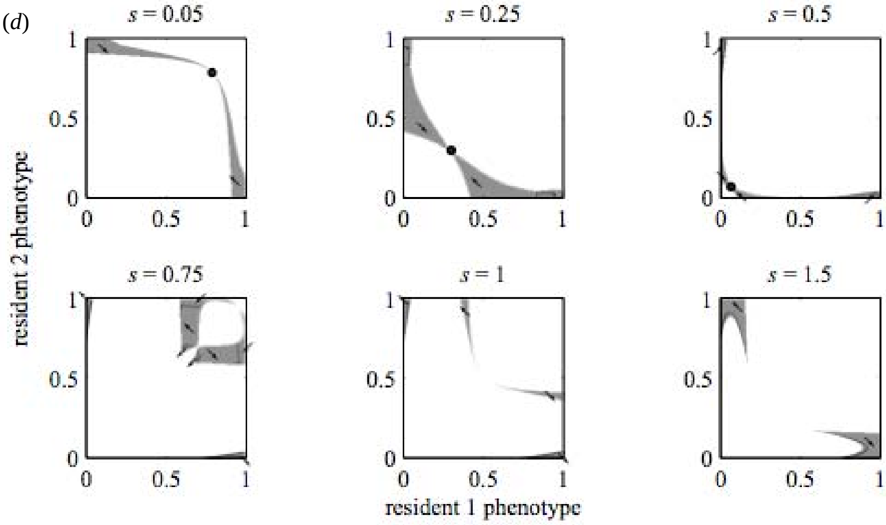

Figure S4

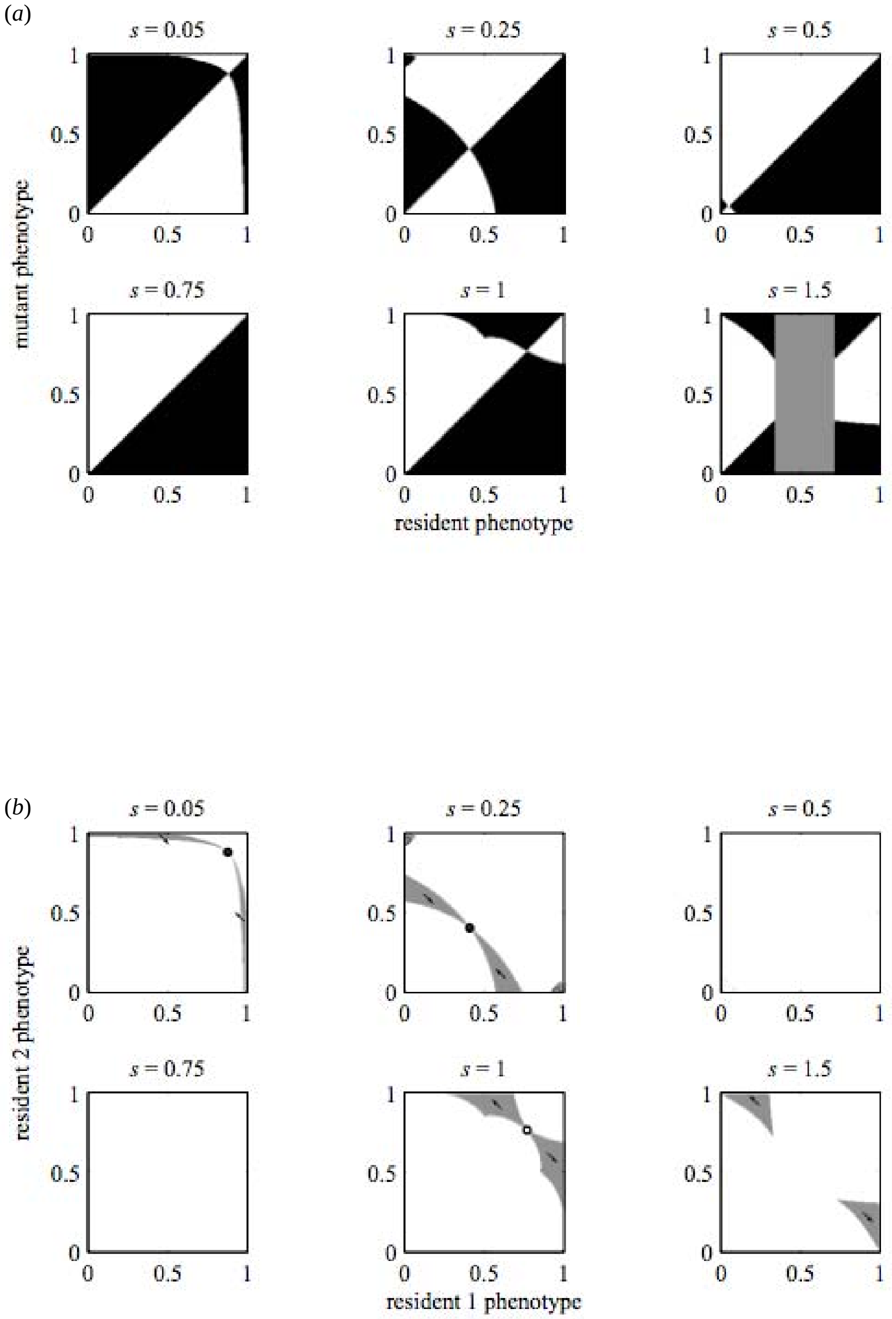
(a)
s = 0.05
s = 0.25
s = 0.5
s = 0.75
s = 1
s = 1.5
mutant phenotype
resident phenotype
0
0.5
1
(b)
s = 0.05
s = 0.25
s = 0.5
s = 0.75
s = 1
s = 1.5
resident 2 phenotype
resident 1 phenotype
0
0.5
1

Figure S5

(*a*)

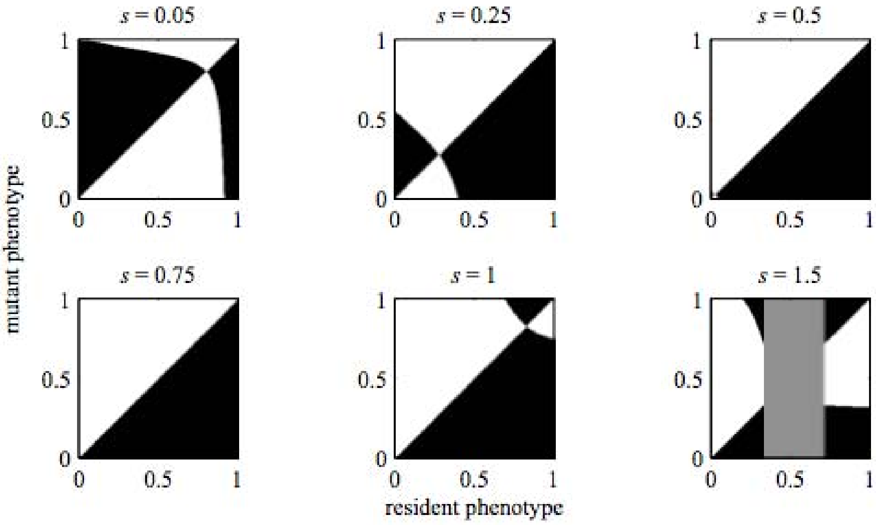
s = 0.05
s = 0.25
s = 0.5
s = 0.75
s = 1
s = 1.5
mutant phenotype
resident phenotype
0
0.5
1

(*b*)

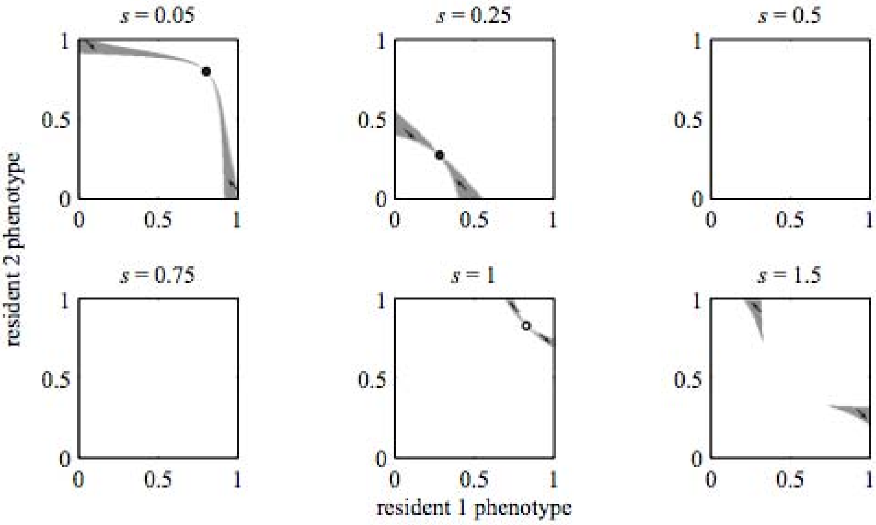
s = 0.05
s = 0.25
s = 0.5
s = 0.75
s = 1
s = 1.5
resident 2 phenotype
resident 1 phenotype
0
0.5
1

Figure S5 (continued)

(*c*)

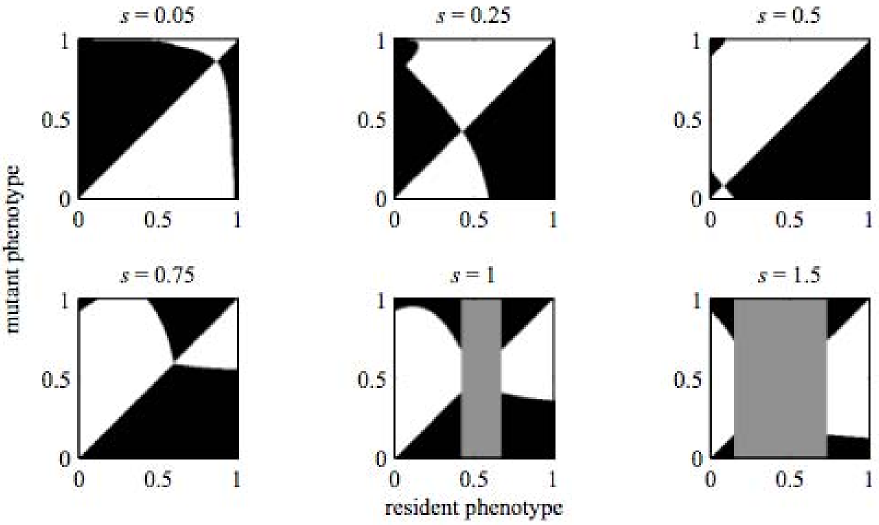

(*d*)

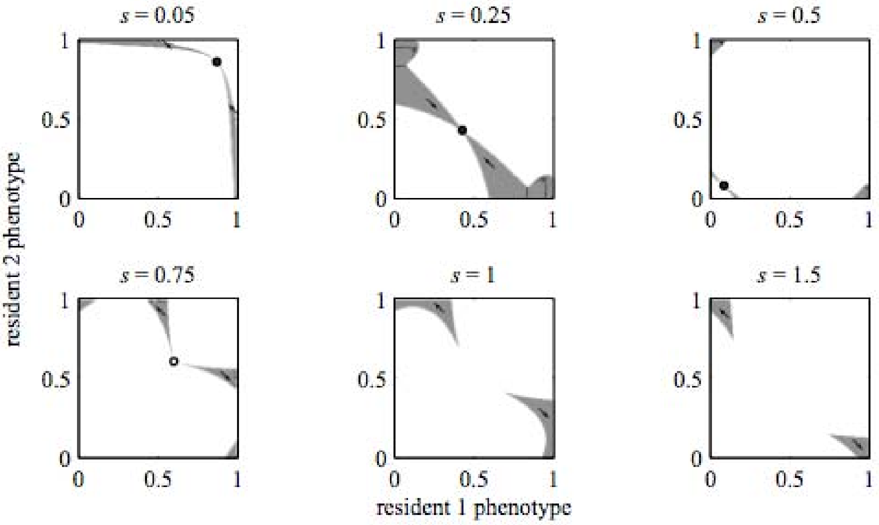

Figure S6

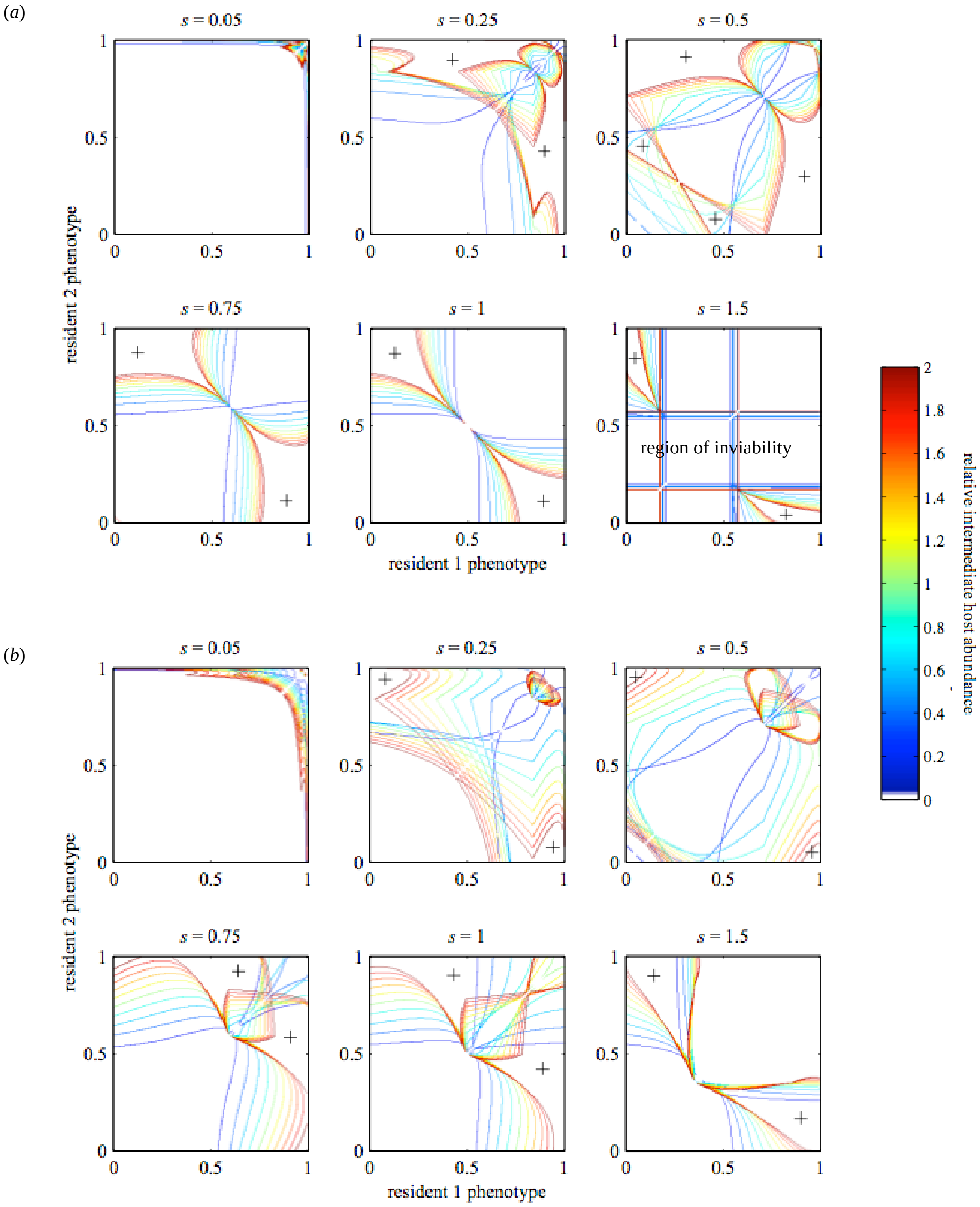
(a)
s = 0.05
s = 0.25
s = 0.5
s = 0.75
s = 1
s = 1.5
region of inviability
resident 2 phenotype
resident 1 phenotype
0
0.5
1
(b)
s = 0.05
s = 0.25
s = 0.5
s = 0.75
s = 1
s = 1.5
resident 2 phenotype
resident 1 phenotype
relative intermediate host abundance
0
0.2
0.4
0.6
0.8
1
1.2
1.4
1.6
1.8
2

Figure S7

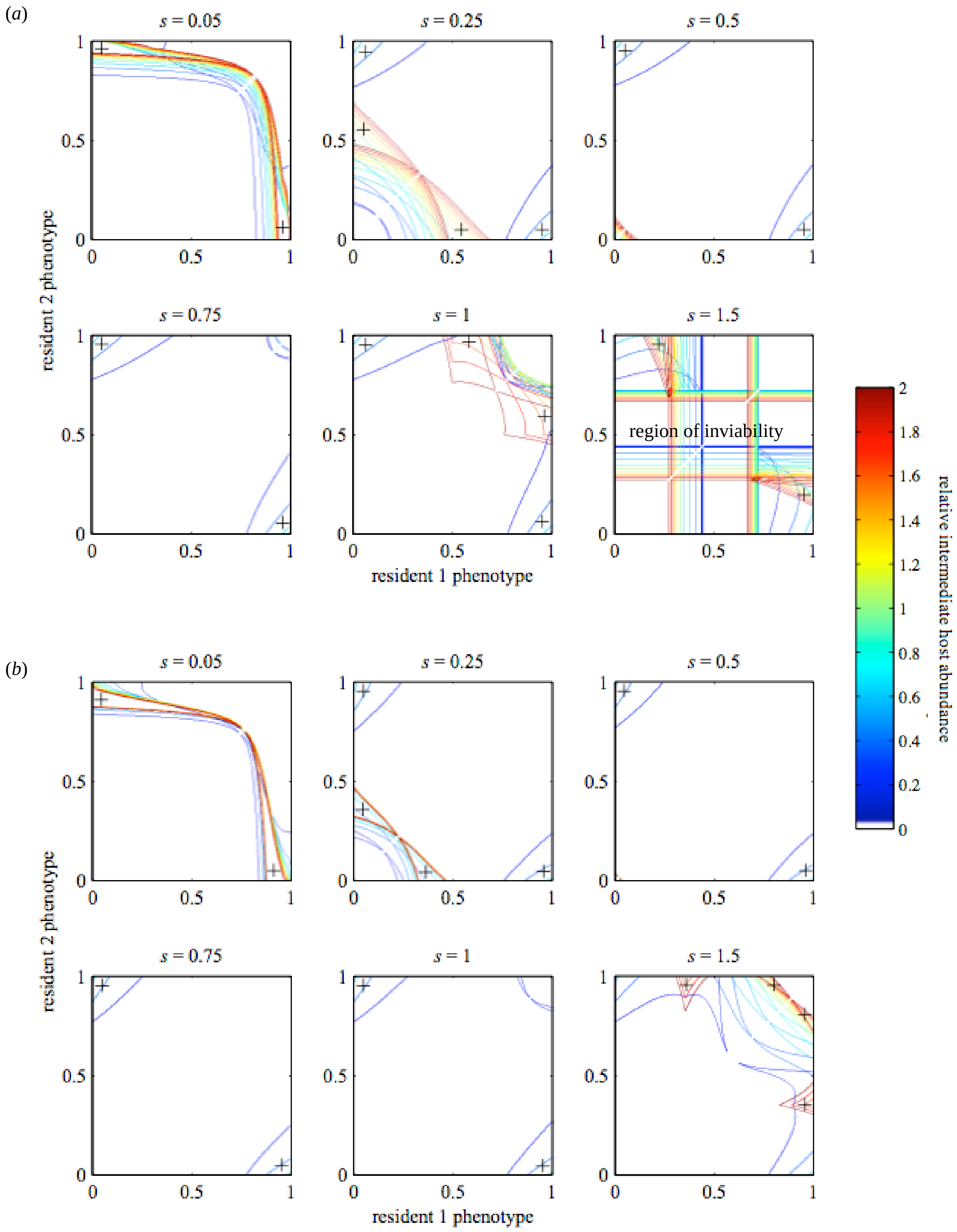
(a)
s = 0.05
s = 0.25
s = 0.5
s = 0.75
s = 1
s = 1.5
region of inviability
resident 2 phenotype
resident 1 phenotype
0
0.5
1
(b)
s = 0.05
s = 0.25
s = 0.5
s = 0.75
s = 1
s = 1.5
resident 2 phenotype
resident 1 phenotype
relative intermediate host abundance
2
1.8
1.6
1.4
1.2
1
0.8
0.6
0.4
0.2
0

Figure S8

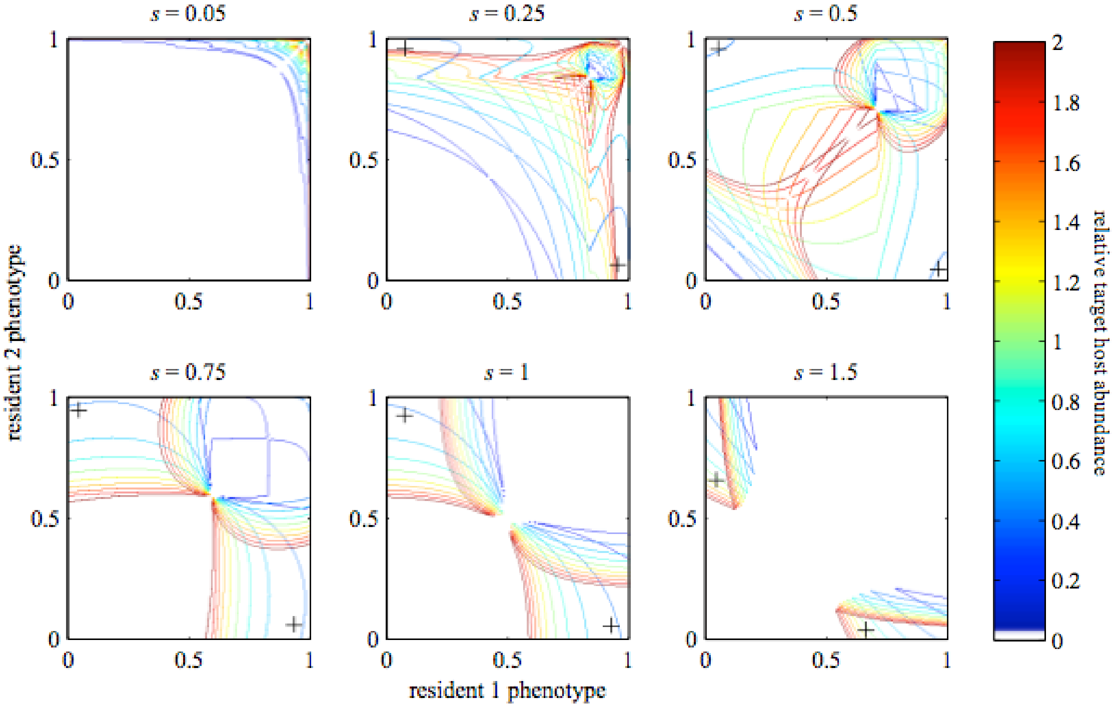
s = 0.05
s = 0.25
s = 0.5
s = 0.75
s = 1
s = 1.5
1
0.5
0
0
0.5
1
resident 2 phenotype
resident 1 phenotype
relative target host abundance
2
1.8
1.6
1.4
1.2
1
0.8
0.6
0.4
0.2
0

Figure S9

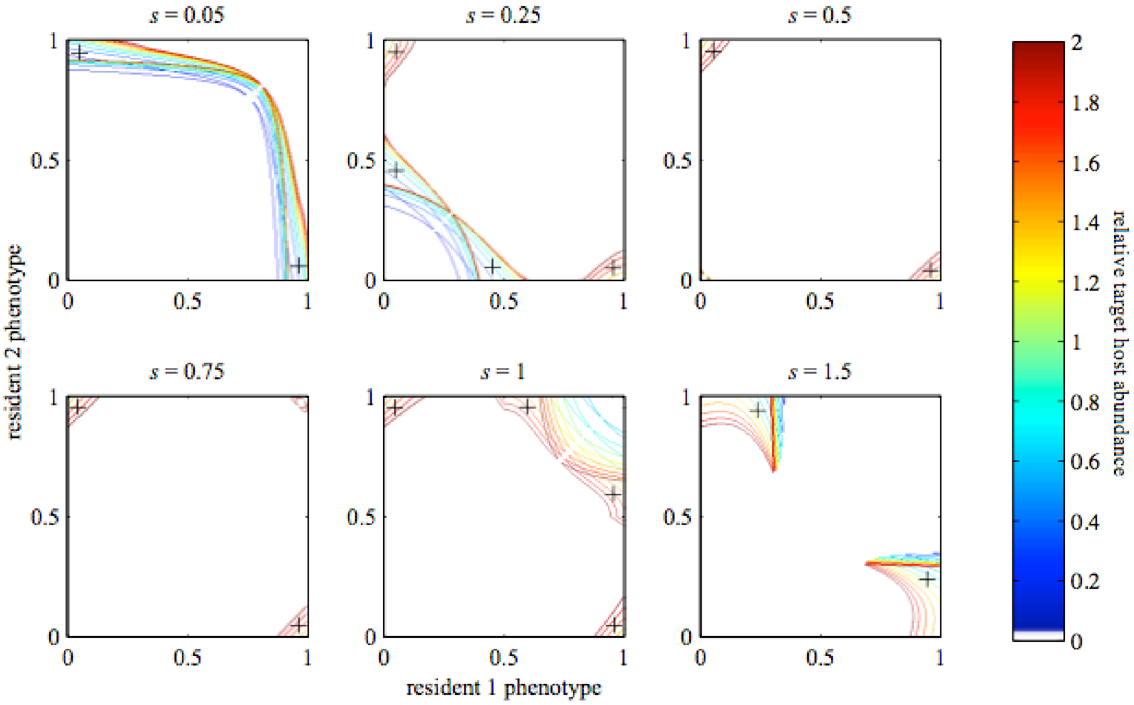
s = 0.05
s = 0.25
s = 0.5
s = 0.75
s = 1
s = 1.5
resident 2 phenotype
resident 1 phenotype
0
0.5
1
relative target host abundance
2
1.8
1.6
1.4
1.2
1
0.8
0.6
0.4
0.2
0

Figure S10

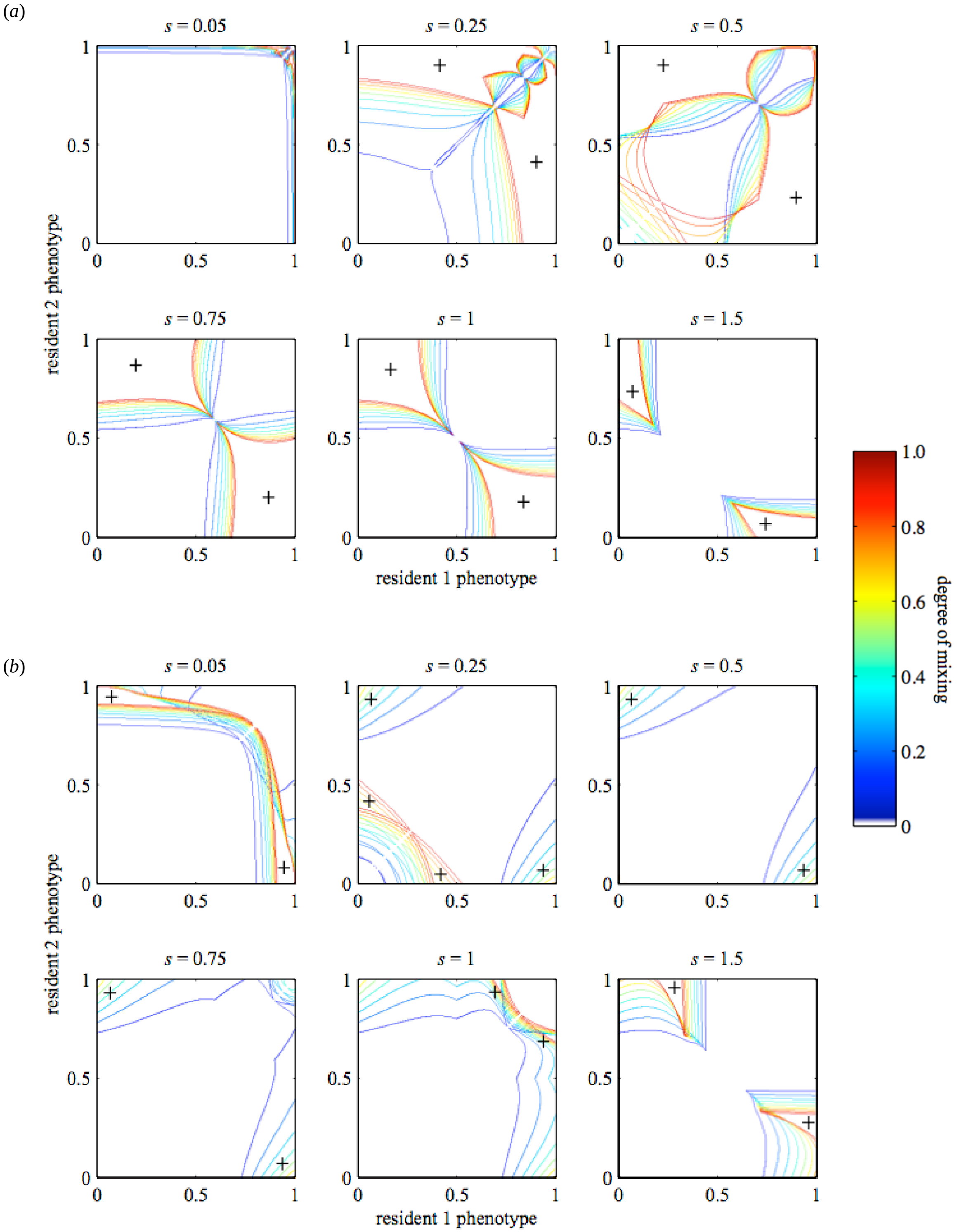
(a)
s = 0.05
s = 0.25
s = 0.5
s = 0.75
s = 1
s = 1.5
resident 2 phenotype
resident 1 phenotype
0
0.5
1
(b)
s = 0.05
s = 0.25
s = 0.5
s = 0.75
s = 1
s = 1.5
resident 2 phenotype
resident 1 phenotype
degree of mixing
1.0
0.8
0.6
0.4
0.2
0

Figure S11

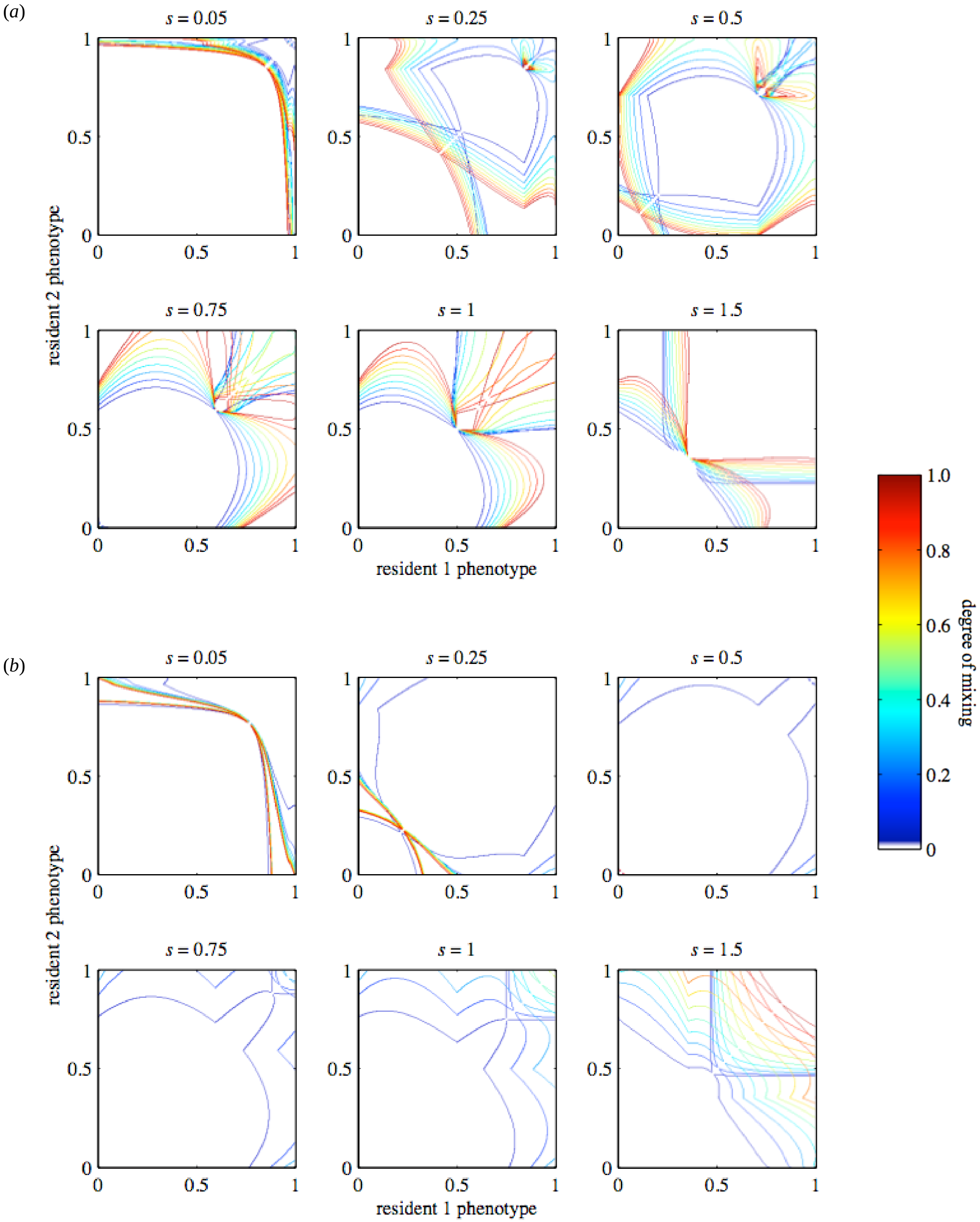
(a)
s = 0.05
s = 0.25
s = 0.5
s = 0.75
s = 1
s = 1.5
resident 2 phenotype
resident 1 phenotype
0
0.5
1
(b)
s = 0.05
s = 0.25
s = 0.5
s = 0.75
s = 1
s = 1.5
resident 2 phenotype
resident 1 phenotype
degree of mixing
1.0
0.8
0.6
0.4
0.2
0

Figure S12

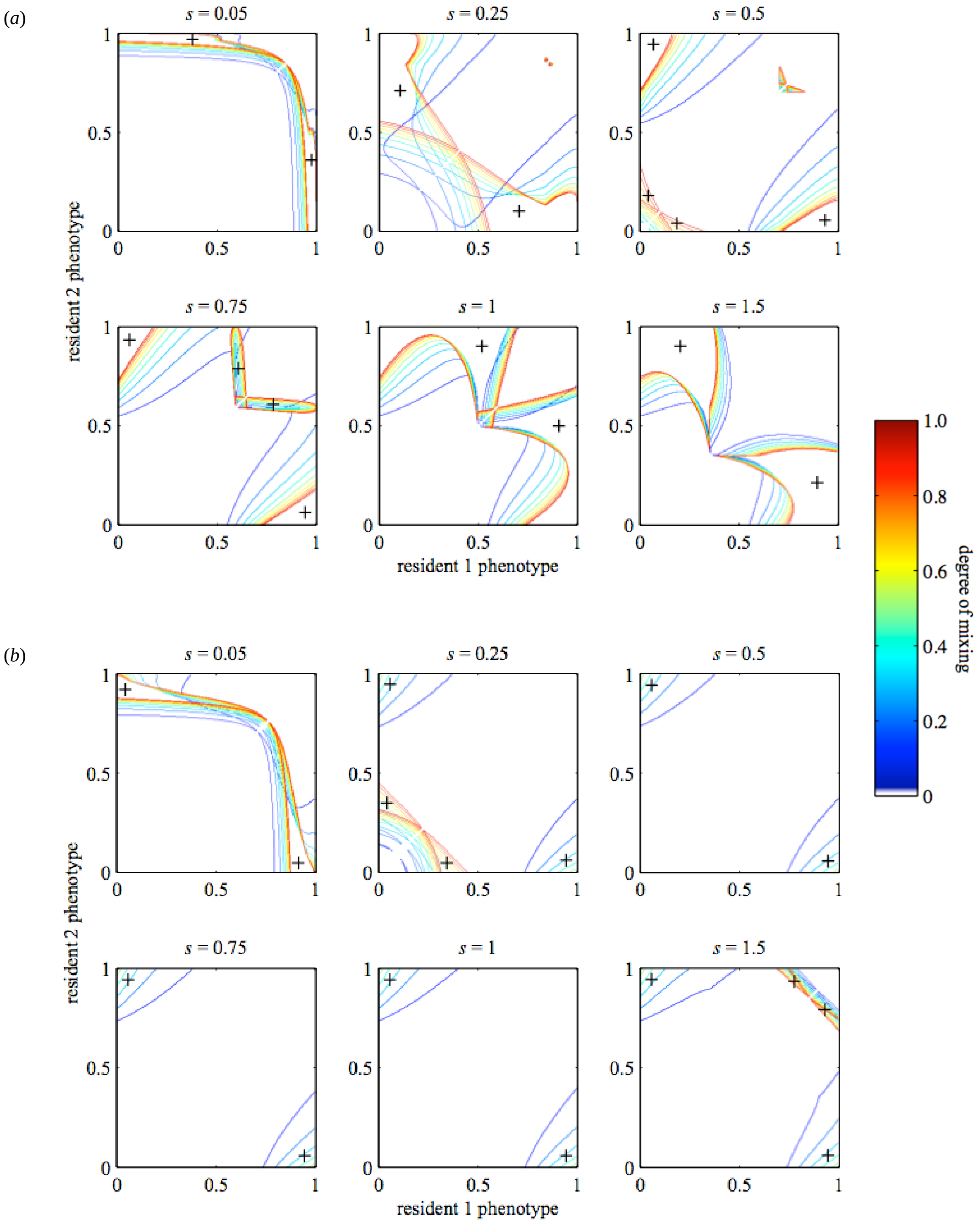
(a)
s = 0.05
s = 0.25
s = 0.5
s = 0.75
s = 1
s = 1.5
resident 2 phenotype
resident 1 phenotype
0
0.5
1
(b)
s = 0.05
s = 0.25
s = 0.5
s = 0.75
s = 1
s = 1.5
resident 2 phenotype
resident 1 phenotype
1.0
0.8
0.6
0.4
0.2
0
degree of mixing

VI. References

Alexander, D. J. 2000 A review of avian influenza in different bird species. *Veterinary Microbiology* **74**, 3-13.

Brown, I. H. 2000 The epidemiology and evolution of influenza viruses in pigs. *Veterinary Microbiology* **74**, 29-46.

Brown, I. H., Harris, P. A. & Alexander, D. J. 1995 Serological Studies of Influenza-Viruses in Pigs in Great-Britain 1991-2. *Epidemiology and Infection* **114**, 511-520

Campitelli, L., Donatelli, I., Foni, E., Castrucci, M. R., Fabiani, C., Kawaoka, Y., Krauss, S. & Webster, R. G. 1997 Continued evolution of H1N1 and H3N2 influenza viruses in pigs in Italy. *Virology* **232**, 310-318.

Carrat, F., Vergu, E., Ferguson, N. M., Lemaitre, M., Cauchemez, S., Leach, S. & Valleron, A. J. 2008 Time lines of infection and disease in human influenza: A review of volunteer challenge studies. *American Journal of Epidemiology* **167**, 775-785.

Halvorson, D., Karunakaran, D., Senne, D., Kelleher, C., Bailey, C., Abraham, a., Hinshaw, V. & Newman, J. 1983 Epizootiology of Avian Influenza - Simultaneous Monitoring of Sentinel Ducks and Turkeys in Minnesota. *Avian Diseases* **27**, 77-85.

Hinshaw, V. S., Webster, R. G., Easterday, B. C. & Bean, W. J. 1981 Replication of Avian Influenza-a Viruses in Mammals. *Infection and Immunity* **34**, 354-361.

Hulse-Post, D. J., Sturm-Ramirez, K. M., Humberd, J., Seiler, J. P., Govorkova, E. A., Krauss, S., Scholtissek, C., Puthavathana, P., Buranathai, C., Nguyen, T. D., Long, H. T., Naipospos, T. S. P., Chen, H., Ellis, T. M., Guan, Y., Peiris, J. S. M. & Webster, R. G. 2005 Role of domestic ducks in the propagation and biological evolution of higthly pathogenic H5N1 influenza viruses in Asia. *Proceedings of the National Academy of Sciences of the United States of America* **102**, 10682-10687.

Karunakaran, D., Hinshaw, V., Poss, P., Newman, J. & Halvorson, D. 1983 Influenza-a Outbreaks in Minnesota Turkeys Due to Subtype-H10N7 and Possible Transmission by Waterfowl. *Avian Diseases* **27**, 357-366.

Kida, H., Yanagawa, R. & Matsuoka, Y. 1980 Duck Influenza Lacking Evidence of Disease Signs and Immune-Response. *Infection and Immunity* **30**, 547-553.

Koopmans, M., Wilbrink, B., Conyn, M., Natrop, G., van der Nat, H., Vennema, H., Meijer, A., van Steenbergen, J., Fouchier, R., Osterhaus, A. & Bosman, A. 2004 Transmission of H7N7 avian influenza A virus to human beings during a large outbreak in commercial poultry farms in the Netherlands. *Lancet* **363**, 587-593.

Leekha, S., Zitterkopf, N. L., Espy, M. J., Smith, T. F., Thompson, R. L. & Sampathkumar, P. 2007 Duration of influenza a virus shedding in hospitalized patients and implications for infection control. *Infection Control and Hospital Epidemiology* **28**, 1071-1076.

Ly, S., Van Kerkhove, M. D., Holl, D., Froehlich, Y. & Vong, S. 2007 Interaction between humans and poultry, rural Cambodia. *Emerging Infectious Diseases* **13**, 130-132.

Myers, K. P., Olsen, C. W., Setterquist, S. F., Capuano, A. W., Donham, K. J., Thacker, E. L., Merchant, J. A. & Gray, G. C. 2006 Are swine workers in the United States at increased risk of infection with zoonotic influenza virus? *Clinical Infectious Diseases* **42**, 14-20.

Olsen, C. W., Brammer, L., Easterday, B. C., Arden, N., Belay, E., Baker, I. & Cox, N. J. 2002 Serologic evidence of H1 swine influenza virus infection in swine farm residents and employees. *Emerging Infectious Diseases* **8**, 814-819.

Olsen, C. W., Carey, S., Hinshaw, L. & Karasin, A. I. 2000 Virologic and serologic surveillance for human, swine and avian influenza virus infections among pigs in the north-central United States. *Archives of Virology* **145**, 1399-1419.

Saenz, R. A., Hethcote, H. W. & Gray, G. C. 2006 Confined animal feeding operations as amplifiers of influenza. *Vector-Borne and Zoonotic Diseases* **6**, 338-346.

Sivanandan, V., Halvorson, D. A., Laudert, E., Senne, D. A. & Kumar, M. C. 1991 Isolation of H13N2 Influenza-a Virus from Turkeys and Surface-Water. *Avian Diseases* **35**, 974-977.

Van der Goot, J. A., de Jong, M. C. M., Koch, G. & van Boven, M. 2003 Comparison of the transmission characteristics of low and high pathogenicity avian influenza A virus (H5N2). *Epidemiology and Infection* **131**, 1003-1013.

Webster, R. G. & Hulse, D. J. 2004 Microbial adaptation and change: avian influenza. *Revue Scientifique et Technique de l'Office International des Epizooties* **23**, 453-465.

Yu, H., Zhang, G. H., Hua, R. H., Zhang, Q., Liu, T. Q., Liao, M. & Tong, G. Z. 2007 Isolation and genetic analysis of human origin H1N1 and H3N2 influenza viruses from pigs in China. *Biochemical and Biophysical Research Communications* **356**, 91-96.